CEBAF

The Continuous Electron Beam Accelerator Facility

Theory Group Preprint Series

Additional copies are available from the authors.

The Southeastern Universities Research Association (SURA) operates the Continuous Electron Beam Accelerator Facility for the United States Department of Energy under contract DE-AC05-84ER40150

MANY-BODY CURRENTS AND THE STRANGE-QUARK CONTENT OF ^{4}He *

M. J. Musolf† and R. Schiavilla

Department of Physics, Old Dominion University
Norfolk, Virginia 23529 U.S.A.
and
CEBAF Theory Group, MS 12H2
Newport News, Virginia 23606 U.S.A.

and

T. W. Donnelly

Center for Theoretical Physics
Laboratory for Nuclear Science
and
Department of Physics
Massachusetts Institute of Technology
Cambridge, Massachusetts 02139 U.S.A.

CEBAF # TH-94-10

April, 1994

*This work is supported in part by funds provided by the U. S. Department of Energy (D.O.E.) under contracts #DE-AC05-84ER40150 and #DE-AC02-76ER03069.

†National Science Foundation Young Investigator

ABSTRACT

Meson-exchange current (MEC) contributions to the parity-violating (PV) asymmetry for elastic scattering of polarized electrons from ^{4}He are calculated over a range of momentum transfer using Monte Carlo methods and a variational ^{4}He ground state wavefunction. The results indicate that MEC's generate a negligible contribution to the asymmetry at low-$|\vec{q}|$, where a determination of the nucleon's mean square strangeness radius could be carried out at CEBAF. At larger values of momentum transfer – beyond the first diffraction minimum two-body corrections from the ρ-π "strangeness charge" operator enter the asymmetry at a potentially observable level, even in the limit of vanishing strange-quark matrix elements of the nucleon. For purposes of constraining the nucleon's strangeness electric form factor, theoretical uncertainties associated with these MEC contributions do not appear to impose serious limitations.

I. Introduction. One objective of the CEBAF physics program is to probe the strange-quark "content" of the nucleon with parity-violating (PV) electron scattering. As discussed elsewhere in the literature [1-7], PV electron scattering at low-to-intermediate energies is particularly suited to the study of strange-quark vector current matrix elements, $\langle H|\bar{s}\gamma_\mu s|H\rangle$, where H is a hadron. In the case where the target is a nucleon ($|H\rangle = |p\rangle$ or $|n\rangle$), this matrix element can parameterized by two form factors, $G_E^{(s)}(Q^2)$ and $G_M^{(s)}(Q^2)$, the strangeness electric and magnetic form factors, respectively. Extractions of $\langle N|\bar{s}s|N\rangle$, the nucleon's strange-quark scalar density, from $\pi - N$ scattering [8,9], as well as determinations of the strange-quark axial vector matrix element, $\langle N|\bar{s}\gamma_\mu\gamma_5 s|N\rangle$, from elastic $\nu_\mu p/\bar{\nu}_\mu p$ scattering [10-12] and measurements of the g_1 sum [13-15], suggest that the strange-quark "sea" plays a more important role in the low-energy properties of the nucleon than one might expect based on the success of valence quark models. Measurements of $\langle N|\bar{s}\gamma_\mu s|N\rangle$ would provide an additional window on the sea-quark structure of the nucleon. Model estimates of $G_E^{(s)}$ and $G_M^{(s)}$ at low-$|Q^2|$ span a wide spectrum in both magnitude and sign [16-21]. It is therefore of interest to extract the strangeness form factors at a level needed to distinguish among model calculations and their attendant physical pictures.

To this end, use of a proton target would not be sufficient. The presence of several poorly-constrained form factors in the PV elastic ^{1}H$(\vec{e},e)$ asymmetry, as well as theoretical uncertainties associated with axial vector radiative corrections, limit the precision with which $G_E^{(s)}$ and $G_M^{(s)}$ could be determined from the proton alone [1,2]. The use of $A > 1$ targets in conjuction with the proton offers the possibility of imposing more stringent limits on the nucleon's s-quark vector current matrix elements [1,2,22] than could be obtained with a proton target only. In this regard, the $(J^\pi, T) = (0^+, 0)$ nuclei, such as ^{4}He, constitute an attractive case, since the ground states of such nuclei can support matrix elements of only one operator – the isoscalar Coulomb operator [1,2,22,23]. In the one-body approximation to this operator, the nuclear wavefunction dependence of the Coulomb matrix elements effectively cancels out from the PV asymmetry for such nuclei, leaving only a sensitivity to Standard Model couplings and single nucleon form factors (*e.g.*, $G_E^{(s)}$). Two approved CEBAF experiments rely on this feature of $A_{LR}(0^+, 0)$, the PV left-right asymmetry [24,25]. The proper interpretation of $A_{LR}(0^+, 0)$ requires that one understand the importance of many-body corrections to the one-body asymmetry. Meson-exchange currents (MEC's) constitute one class of such many-body effects. In previous work [26], we computed MEC contributions to the ^{4}He mean-square "strangeness radius", which generates the leading s-quark contribution to $A_{LR}(^4\text{He})$ at low-$|\vec{q}|$. The results of

that calculation, peformed with a simple ^{4}He shell model wavefunction and phenomenological two-body correlation function, indicate that the ^{4}He strangeness radius is dominated by strange-quarks inside the nucleon.

In the present work, we extend the calculation of Ref. [26] using a ^{4}He variational wavefunction obtained from realistic interactions and computing the asymmetry over the full range of momentum transfer germane to the future CEBAF experiments. Our results indicate that the ^{4}He strangeness radius is two orders of magnitude more sensitive to the nucleon's strangeness radius than to two-body contributions. At the higher $|\vec{q}|$ of experiment [24], the situation is more complex. Even if the nucleon matrix element $\langle N|\bar{s}\gamma_\mu s|N\rangle$ were to vanish, the PV asymmetry would still receive a non-negligible contribution from non-nucleonic s-quark matrix elements. In particular, the $\rho-\pi$ strangeness transition charge operator generates nearly a 15% contribution to the asymmetry at the kinematics of the experiment [24]. In this case, an experiment like that of Ref. [24] would be significant in two respects. First, it would be interesting to measure a non-negligible strange-quark matrix element in a strongly-interacting, non-strange system, regardless of the dynamical origin of that matrix element. Second, the only other observable with significant sensitivity to the $\rho-\pi$ MEC is the B form factor of the deuteron [27]. If, however, $G_E^{(s)}$ and $G_M^{(s)}$ are non-zero, the level of theoretical ***uncertainty*** associated with the present MEC calculation does not appear to be large enough to significantly weaken the possible constraints on $G_E^{(s)}$ which a measurement of $A_{LR}(^4\mathrm{He})$ could provide.

In the remainder of the paper we provide details of the calculations leading to these conclusions. Section II gives our formalism, including expressions for the operators used. In section III, we treat the computation of the ^{4}He matrix elements of these operators, considering first the simple case of a shell model ground state and subsequently turning to the Variational Monte Carlo (VMC) approach. In section IV we discuss our results, including implications for the interpretation of $A_{LR}(^4\mathrm{He})$ and studies of nucleonic strangeness. Technical details may be found in the Appendix.

II. Formalism. The PV left-right asymmetry for scattering of polarized electrons from a nuclear target depends on the interference of the electromagnetic (EM) and PV weak neutral current (NC) amplitudes, M_{EM} and M_{NC}^{PV}, as

$$A_{LR} \approx \frac{2\mathrm{Re}\; M_{EM}^* M_{NC}^{PV}}{|M_{EM}|^2} \quad , \tag{1}$$

where $|M_{EM}| >> |M_{NC}^{PV}|$ at low energies. The amplitude M_{NC}^{PV} is proportional to the sum of two terms,

$$\ell_{NC}^{\mu} J_{\mu 5}^{NC} + \ell_{NC}^{\mu 5} J_{\mu}^{NC} \quad , \tag{2}$$

where $\ell_{NC}^{\mu(5)}$ is the electron's vector (axial vector) neutral current and $J_{\mu(5)}^{NC}$ is the nucleon or nuclear matrix element of the hadronic vector (axial vector) NC. One may rewrite A_{LR} in terms of quantities which set the scale of the asymmetry and a ratio of nuclear response functions [1,2]

$$A_{LR} = \frac{G_\mu Q^2}{2\sqrt{2}\pi\alpha} \frac{W^{PV}}{F^2} \quad , \tag{3}$$

where G_μ is the Fermi constant measured in muon-decay, α is the EM fine structure constant, and $Q^2 = \omega^2 - q^2$ with ω and $q = |\vec{q}|$ being the energy and magnitude of three-momentum transfer to the target. The response functions appearing in the ratio of Eq. (3) may be written as

$$F^2 = v_L R_L + v_T R_T \tag{4a}$$

$$W^{PV} = v_L W_{AV}^L + v_T W_{AV}^T + v_{T'} W_{VA}^{T'} \quad , \tag{4b}$$

where v_L, v_T and $v_{T'}$ are leptonic kinematic factors; R_L and R_T are the usual longitudinal and transverse EM response functions; and $W_{AV}^{L,T}$ and $W_{VA}^{T'}$ are analogous PV response functions involving products of the hadronic EM and vector NC ("AV") or axial vector NC ("VA") [1,2].

In this work, we follow the approach taken in Refs. [1-7] and keep only the three lightest quarks in the hadronic current. In this case, one has for the two vector currents

$$J_\mu^{EM} = J_\mu^{EM}(T=1) + J_\mu^{EM}(T=0) \tag{5a}$$

$$J_\mu^{NC} = \xi_V^{T=1} J_\mu^{NC}(T=1) + \sqrt{3}\xi_V^{T=0} J_\mu^{EM}(T=0) + \xi_V^{(0)} \bar{s}\gamma_\mu s \quad , \tag{5b}$$

where the $J_\mu^{EM}(T)$ are the isovector ($T=1$) and isoscalar ($T=0$) EM currents and the $\xi_V^{(a)}$ are couplings determined by the Standard Model [1,2,22]. A decomposition of $J_{\mu 5}^{NC}$ analogous to that of Eq. (5b) but involving the SU(3) octet of axial currents and $\bar{s}\gamma_\mu\gamma_5 s$ may also be made [1,2,7]. Since the ^{4}He ground state supports no axial vector matrix element, however, we do not consider $J_{\mu 5}^{NC}$ further in this work.

In the limit that the ^{4}He ground state is an eigenstate of isospin, the "hadronic ratio" for this target is

$$\frac{W^{PV}}{F^2} = -\frac{1}{2}\left\{\sqrt{3}\xi_V^{T=0} + \xi_V^{(0)} \frac{F_{C0}^{(s)}(q)}{F_{C0}^{T=0}(q)}\right\} \quad . \tag{6}$$

Here, $\sqrt{3}\xi_V^{T=0} = -4\sin^2\theta_W$ and $\xi_V^{(0)} = -1$ at tree level in the Standard Model [1,2,22]. The form factors are given by

$$F_{C0}^{(a)}(q) = \langle 0^+0|\hat{M}_{00}^{(a)}(q)|0^+0\rangle \tag{7a}$$

$$\hat{M}_{00}^{(a)}(q) = \int d^3x\; j_0(qx)Y_{00}(\Omega_x)\hat{\rho}^{(a)}(\vec{x}) \tag{7b}$$

$$= \frac{1}{4\pi}\int d\Omega_q\; Y_{00}(\Omega_q)\hat{\rho}^{(a)}(\vec{q}) \quad , \tag{7c}$$

where $x = |\vec{x}|$ and $\hat{\rho}^{(a)}(\vec{x})$ ($\hat{\rho}^{(a)}(\vec{q})$) denotes the co-ordinate-space (momentum-space) charge ($\mu = 0$) component of either the isoscalar EM current ($(a) \to T = 0$) or strange quark current ($(a) \to (s)$). Matrix elements of the Coulomb operator are simply related to the elastic charge form factor as

$$F_C^{(a)}(q) = \langle 0^+0|\hat{\rho}(\vec{q})|0^+0\rangle = 2\sqrt{\pi}F_{C0}^{(a)}(q) \quad . \tag{7d}$$

One observes from Eq. (6) that were the nuclear matrix elements of $\hat{M}_{00}^{(s)}(q)$ to vanish, the asymmetry would be nominally independent of the details of the nuclear wavefunction.[1] The reason is that (i) in the absence of strangeness, the hadronic isoscalar EM and isoscalar NC currents are identical, up to the overall electroweak coupling, $\sqrt{3}\xi_V^{T=0}$, (ii) isovector matrix elements vanish if the ^{4}He ground state is assumed to be a pure $T = 0$ state, and (iii) a spin-0 ground state cannot support axial vector matrix elements.

One-body operators

Expressions for the one-body charge operators may be obtained starting from Lorentz-covariant forms of the single-nucleon vector current matrix element:

$$\langle N(p')|V_\mu(0)|N(p)\rangle = \bar{U}(p')\left[F_1(Q^2)\gamma_\mu + \frac{iF_2(Q^2)}{2m_N}\sigma_{\mu\nu}Q^\nu\right]U(p) \quad , \tag{8}$$

where F_1 and F_2 are the standard Dirac and Pauli form factors of the nucleon, $U(p)$ and $U(p')$ are nucleon spinors corresponding to nucleon states $|N(p)\rangle$ and $|N(p')\rangle$, respectively, and $V_\mu(\vec{x})$ is any one of the vector currents of interest (isoscalar EM or strangeness). Expanding the right side of Eq. (8) in powers of p/m_N, transforming to co-ordinate space, and summing over all nucleons gives for the $\mu = 0$ component

[1] Apart from contributions from nuclear dispersion corrections; see, *e.g.* Refs. [1,2,22].

$$\hat{\rho}^{(a)}(\vec{q})[1] = \sum_{k=1}^{A} e^{i\vec{q}\cdot\vec{x}_k}\left[\frac{G_E^{(a)}(\tau)}{\sqrt{1+\tau}} - \frac{i}{8m_N^2}\left\{G_E^{(a)}(\tau) - 2G_M^{(a)}(\tau)\right\}\vec{\sigma}_k\cdot\vec{q}\times\vec{P}_k\right] \quad , \tag{9}$$

where $\tau \equiv -Q^2/4m_N^2 = q^2/4m_N^2$ for elastic scattering in the Breit frame, $\vec{P}_k = \vec{p}_k + \vec{p}'_k$, and

$$G_E^{(a)} = F_1^{(a)} - \tau F_2^{(a)} \tag{10a}$$

$$G_M^{(a)} = F_1^{(a)} + F_2^{(a)} \tag{10b}$$

are the Sachs electric (10a) and magnetic (10b) form factors [28]. In arriving at the expression in Eq. (9), we have used the spinor normalization of Ref. [29]. Had we followed the convention of Ref. [30], the charge operator would have contained an additional term Δ_k inside the square brackets given by

$$\Delta_k = \frac{1}{4m_N^2}\left(p_k^2 + p'^2_k\right)(1+\tau)^{-1}\left[G_E^{(a)}(\tau) + \tau G_M^{(a)}(\tau)\right] \quad . \tag{11}$$

Following the convention in Refs. [1-4], we parameterize the momentum-dependence of the one-body form factors as

$$G_E^p(\tau) = G_V^D(\tau) \tag{12a}$$

$$G_M^p(\tau) = \mu_p G_V^D(\tau) \tag{12b}$$

$$G_E^n(\tau) = -\mu_n\tau G_V^D(\tau)\xi_n(\tau) \tag{12c}$$

$$G_M^n(\tau) = \mu_n G_V^D(\tau) \tag{12d}$$

$$G_E^{(s)}(\tau) = \rho_s\tau G_V^D(\tau)\xi_s(\tau) \tag{12e}$$

$$G_M^{(s)}(\tau) = \mu_s G_V^D(\tau) \tag{12f}$$

with

$$G_V^D(\tau) = (1 + \lambda_V^D\tau)^{-2} \tag{13a}$$

$$\xi_n = (1 + \lambda_n\tau)^{-1} \tag{13b}$$

$$\xi_s = (1 + \lambda_E^{(s)}\tau)^{-1} \tag{13c}$$

and

$$G_{E,M}^{T=0} = \frac{1}{2}\left[G_{E,M}^{p} + G_{E,M}^{n}\right] \tag{14a}$$

$$G_{E,M}^{T=1} = \frac{1}{2}\left[G_{E,M}^{p} - G_{E,M}^{n}\right] \quad . \tag{14b}$$

Numerically, one has $\mu_p = 2.79$, $\mu_n = -1.91$, $\lambda_V^p = 4.97$, and $\lambda_n = 5.6$. The rationale for adopting this parameterization is discussed more fully in Refs. [1,2]. The parameters μ_s and ρ_s, which define the strangeness magnetic moment and strangeness radius, respectively, as well as $\lambda_E^{(s)}$ which governs the next-to-leading Q^2 behavior of $G_E^{(s)}$, are presently unknown. One goal of the SAMPLE experiment [6] and up-coming CEBAF experiments [24,25,31] is to place limits on these parameters.

The one-body contribution to the Coulomb multipole operator, obtained by substituting the expression for the charge operator of Eq. (9) into Eq. (7b), is

$$\hat{M}_{00}^{(a)}(q)^{[1]} = \frac{1}{2\sqrt{\pi}}\sum_{k=1}^{A}\left\{\frac{G_E^{(a)}(\tau)}{\sqrt{1+\tau}} j_0(qx_k) + \left[G_E^{(a)}(\tau) - 2G_M^{(a)}(\tau)\right]\frac{q}{2m_N}\frac{j_1(qx_k)}{m_N x_k}\vec{\sigma}_k \cdot \vec{L}_k\right\} \quad , \tag{15}$$

where we have assumed $q_0 = 0$ so that $q^2 = 4m_N^2\tau$ and where $\vec{L}_k$ is the orbital angular momentum of the k-th nucleon. Note that in the limit that the ^{4}He ground state consists of nucleons in S-states only, the spin-orbit operator in $\hat{M}_{00}^{(a)}(q)^{[1]}$ will not contribute to $F_{C0}^{(a)}(q)$. In this case, the Coulomb matrix elements for the isoscalar EM and strangeness charge operators are identical, apart from the single nucleon form factors, rendering their ratio independent of nuclear structure:

$$\left.\frac{F_{C0}^{(s)}(q)^{[1]}}{F_{C0}^{T=0}(q)^{[1]}}\right|_{\text{S-waves}} \longrightarrow \frac{G_E^{(s)}(\tau)}{G_E^{T=0}(\tau)} \quad . \tag{16}$$

However, the presence of a significant D-wave component (the associated probability is about 16% for the variational ^{4}He wavefunction discussed below) implies some level of structure-dependence in the one-body form factor ratio of Eq. (16). For most values of momentum transfer, the magnitude of this structure-dependence is negligible (see the spin-orbit contributions in Figs. 2b and 3b).

Two-body operators

In the one boson-exchange (OBE) approximation, the leading two-body MEC corrections to the one-body result of Eq. (16) are generated by the processes in Fig. 1. The π-exchange and vector meson-exchange "pair currents" (Figs. 1a,b) are familiar from previous work on MEC's [32-36], as is the pseudoscalar-vector meson "transition current" of Fig. 1c. In each case, the isoscalar EM and strangeness two-body currents have the same structure, apart from the form factors appearing at the $N\bar{N}$ creation/annihilation vertex and $V-\pi$ transition vertex. The ^{4}He elastic from factors receive no contribution from processes in which a virtual γ or Z^0 couples to an exchanged pseudoscalar or vector meson. The reason is that matrix elements of the form $\langle M|V_\mu(0)|M'\rangle$ must vanish in order to respect G-parity invariance when $|M'\rangle$ and $|M\rangle$ are identical meson states (apart from momenta) and when V_μ is either $J_\mu^{EM}(T=0)$ or $\bar{s}\gamma_\mu s$. Moreover, one has no contribution from an $\omega-\pi$ transition current since currents which are strong isoscalar operators cannot induce such an isospin-changing transition. We have not included contributions from isobar currents, since the lightest nucleon resonance accessible with an isoscalar current is the $N(1440)$. We assume contributions from the associated current are suppressed by the large mass difference between this state and the nucleon.

We derive two-body charge operators by computing the covariant momentum-space Feynman amplitudes associated with the diagrams in Fig. 1, peforming the standard non-relativistic reduction, and transforming to co-ordinate space. We take the meson-nucleon couplings from the conventional low-energy effective Lagrangians:

$$\mathcal{L}_{NN\pi} = \frac{g_{\pi NN}}{2m_N}\bar{\psi}_N(x)\not{D}\vec{\pi}(x)\cdot\vec{\tau}\psi_N(x) \tag{17a}$$

$$\mathcal{L}_{NN\rho} = g_{\rho NN}\bar{\psi}_N(x)\left[\gamma^\mu + \frac{\kappa_\rho}{2m_N}\sigma^{\mu\nu}\partial_\nu\right]\vec{\rho}_\mu\cdot\vec{\tau}\psi_N(x) \tag{17b}$$

$$\mathcal{L}_{NN\omega} = g_{\omega NN}\bar{\psi}_N(x)\left[\gamma^\mu + \frac{\kappa_\omega}{2m_N}\sigma^{\mu\nu}\partial_\nu\right]\omega_\mu\psi_N(x) \tag{17c}$$

and

$$D^\mu = \partial^\mu + ie\hat{Q}_{EM}A^\mu + ig\hat{Q}_W Z^\mu \quad , \tag{17d}$$

where ψ_N is a nucleon field, π^a, ρ_μ^a, and ω_μ are the pion, rho-meson, and omega-meson fields, respectively, "a" is an isospin index, g is the semi-weak coupling, $\hat{Q}_{EM}$ and $\hat{Q}_W$ are the EM and weak NC charge operators, and A^μ and Z^μ are the photon and Z^0 fields, respectively. We take the couplings appearing in Eq. (17)

to have the values $g_{\pi NN} = 13.6$, $g_{\rho NN} = 2.6$, $g_{\omega NN} = 14.6$, $\kappa_\rho = 6.6$, and $\kappa_\omega = -0.12$ [37]. Momentum-space matrix elements of the operators in Eq. (17) have the same structure as the effective Lagrangians, but with the nucleon fields replaced by plane wave spinors, the derivatives replaced by ik^μ, where k^μ is the momentum of the outgoing meson, and the vector boson fields replaced by the corresponding polarization vectors, ε_μ. For the $\rho - \pi$ transition current matrix element one has

$$\langle \pi^b(k_2)|V_\mu^{(a)}(0)|\rho^c(k_1,\varepsilon)\rangle = -\frac{g_{\rho\pi}^{(a)}(Q^2)}{m_\rho}\delta_{bc}\epsilon_{\mu\nu\alpha\beta}k_1^\nu k_2^\alpha \varepsilon^\beta \quad , \tag{18}$$

where as usual "a" denotes either the EM or strange-quark current [38]. In the case of the former, the value of the transition form factor at the photon point is known to be $g_{\rho\pi}^{T=0}(Q^2=0) \equiv g_{\rho\pi\gamma} = 0.56$ [39], while the Q^2-dependence may be modelled using ω-pole dominance:

$$g_{\rho\pi}^{T=0}(Q^2) = g_{\rho\pi\gamma}\left(1 - Q^2/m_\omega^2\right)^{-1} \quad . \tag{19}$$

In the case where $V_\mu^{(a)} = \bar{s}\gamma_\mu s$, one may follow a similar approach and assume ϕ-meson dominance, which is reasonable since the ϕ is almost pure $s\bar{s}$:

$$g_{\rho\pi}^{(s)}(Q^2) = g_{\rho\pi s}\left(1 - Q^2/m_\phi^2\right)^{-1} \quad . \tag{20}$$

The measured rates for $\phi \to \rho\pi$ and $\phi \to \ell^+\ell^-$ (ℓ is a charged lepton) can be used to estimate the value of this form factor at $Q^2 = 0$ to be $|g_{\rho\pi s}| = 0.26$ [40].

Before proceeding, we touch on one issue associated with the vector meson pair current operators. These operators are derived by keeping only the negative-energy pole of the nucleon propagator, as shown in Fig. 1. The resulting two-body nuclear matrix element is thus distinct from the matrix element containing the positive energy pole, which contributes via the full nuclear Green's function in time-ordered perturbation theory:

$$\sum_n \left[\frac{\langle f|J_\mu|n\rangle\langle n|\hat{H}_{NUC}|i\rangle}{E_i - E_n + i\epsilon} + \frac{\langle f|\hat{H}_{NUC}|n\rangle\langle n|J_\mu|i\rangle}{E_i - E_n + i\epsilon}\right] \quad . \tag{21}$$

Here, $\hat{H}_{NUC}$ is the full nuclear Hamiltonian and (i, f, n) denote initial, final, and intermediate nuclear states, respectively. Following this prescription leads one to a two-body pair-current operator having the same form as given in Ref. [36]. It has been argued, however, that one must include an additional retardation contribution arising from the positive-energy pole in the nucleon propagator whose residue contains a dependence on the energy transfer between the two nucleons.

Inclusion of this additional term results in the form for the pair-current charge operator given in Refs. [32,33]. Rather than attempting to choose between these two approaches, we compute $F_{C0}^{(s)}$ in two ways – once using each of these two prescriptions – in order to determine the impact of this choice. As we note in Section IV, the vector-meson exchange contributions to the ^{4}He form factors are sufficiently small in comparison with other contributions that the impact of this choice in the value for $F_{C0}^{(s)}$ is insignificant.

The momentum-space charge operators for the pair currents are

$$\hat{\rho}(\vec{p}_1,\vec{p}_1',\vec{p}_2,\vec{p}_2';\vec{q})^{[2]}_{\rm pionic} = (2\pi)^3\delta(\vec{k}_1+\vec{k}_2-\vec{q})\left[\frac{g_{\pi NN}^2}{4m_N^3}\right]F_1^{(i)}(\tau)\vec{\tau}_1\cdot\vec{\tau}_2 \tag{22a}$$
$$\times\left\{\frac{1}{\vec{k}_2^2+m_\pi^2}\vec{\sigma}_1\cdot\vec{q}\,\vec{\sigma}_2\cdot\vec{k}_2 + (1\leftrightarrow 2)\right\} \quad ,$$

where $\vec{k}_i = \vec{p}_i' - \vec{p}_i$, $i = 1, 2$, and

$$\hat{\rho}(\vec{p}_1,\vec{p}_1',\vec{p}_2,\vec{p}_2';\vec{q})^{[2]\,({\rm a})}_{\rm V-pair} = (2\pi)^3\delta(\vec{k}_1+\vec{k}_2-\vec{q})\left[\frac{g_{VNN}^2}{4m_N^3}\right]G_M^{(i)}(\tau)\hat{T}_V(1,2) \tag{22b}$$
$$\times\left\{\frac{1}{\vec{k}_2^2+m_V^2}\left[(1+\kappa_V)\left(\vec{q}\cdot\vec{k}_2 + \vec{\sigma}_1\times\vec{q}\cdot\vec{\sigma}_2\times\vec{k}_2\right)\right.\right.$$
$$\left.\left. -i\vec{\sigma}_1\times\vec{q}\cdot(\vec{p}_2+\vec{p}_2')\right] + (1\leftrightarrow 2)\right\}$$

excluding the retardation correction or

$$\hat{\rho}(\vec{p}_1,\vec{p}_1',\vec{p}_2,\vec{p}_2';\vec{q})^{[2]\,({\rm b})}_{\rm V-pair} = (2\pi)^3\delta(\vec{k}_1+\vec{k}_2-\vec{q})\left[\frac{g_{VNN}^2}{4m_N^3}\right]\hat{T}_V(1,2) \tag{22c}$$
$$\times\left\{\frac{1}{\vec{k}_2^2+m_V^2}\left[\left((1+\kappa_V)^2F_1^{(i)}(\tau) + (1+\kappa_V)F_2^{(i)}(\tau)\right)\vec{\sigma}_1\times\vec{q}\cdot\vec{\sigma}_2\times\vec{k}_2\right.\right.$$
$$\left.\left. +G_M^{(i)}(\tau)\left((1+\kappa_V)\vec{q}\cdot\vec{k}_2 - i\vec{\sigma}_1\times\vec{q}\cdot(\vec{p}_2+\vec{p}_2')\right)\right] + (1\leftrightarrow 2)\right\}$$

including the retardation term, with

$$\hat{T}_V(1,2) = \begin{cases} \vec{\tau}_1\cdot\vec{\tau}_2\,, & V=\rho \\ 1\,, & V=\omega \end{cases} \tag{23}$$

and where "(i)" indicates either the isoscalar EM or strange-quark charge operators. We have not included the isovector parts of the charge operators. For the transition operators, one has

$$\hat{\rho}(\vec{p}_1,\vec{p}_1',\vec{p}_2,\vec{p}_2';\vec{q})^{[2]}_{\rho\pi} = i(2\pi)^3\delta(\vec{k}_1+\vec{k}_2-\vec{q})\left[\frac{g_{\pi NN}g_{\rho NN}g^{(s)}_{\rho\pi}(Q^2)}{4m_\rho m_N^2}\right]\vec{\tau}_1\cdot\vec{\tau}_2 \qquad (24)$$

$$\times\left\{\frac{1}{(\vec{k}_1^2+m_\pi^2)(\vec{k}_2^2+m_\rho^2)}\vec{\sigma}_1\cdot\vec{k}_1\Big[(\vec{p}_1+\vec{p}_1')\cdot(\vec{k}_1\times\vec{k}_2)\right.$$

$$\left.-i(1+\kappa_\rho)(\vec{k}_1\times\vec{k}_2)\cdot(\vec{k}_2\times\vec{\sigma}_2)\Big]+(1\leftrightarrow 2)\right\} \quad .$$

Expressions for the co-ordinate space forms of the two-body charge operators, $\hat{\rho}(\vec{x}_1,\vec{x}_1',\vec{x}_2,\vec{x}_2';\vec{q})^{[2]}$, as well as for their Coulomb multipole projections, $\hat{M}_{00}(\vec{q})^{[2]}$, are somewhat involved and may be found in the Appendix. For purposes of discussion, it is useful to consider the leading-q behavior of the two-body Coulomb operators (shown in Eqs. (A.10) of the Appendix), since their matrix elements contribute to the ^{4}He EM and strangeness radii. From the low-q expressions for the two-body Coulomb operators, we observe that they vanish at least as rapidly as q^2 for small q. The operators must vanish at $q^2=0$, since the two-body operators cannot change the overall charge (EM or strangeness) of the ^{4}He nucleus. In the case of strangeness, the entire nuclear form factor $F^{(s)}_{C0}$ must vanish at $q^2=0$, since the nucleus has no net strangeness. Thus, in analogy with the single nucleon case, we define a nuclear strangeness radius as

$$\rho_s[\mathrm{nuc}] = 2\sqrt{\pi}\frac{dF^{(s)}_{C0}}{d\tau}\bigg|_{\tau=0} \quad . \qquad (25)$$

Under this definition, $\rho_s[\mathrm{nuc}] = A\rho_s$ in the one-body limit neglecting the spin-orbit contribution. From the expressions in Eq. (A.10), we note that the pionic operator (Eq. (A.10a)) contributes to $F^{(s)}_{C0}$ at $\mathcal{O}(q^4)$, since this operator is proportional to $q^2F_1^{(a)}$ and since $F_1^{(a)}$ vanishes as q^2 for small q. Consequently, the longest-range MEC does not contribute to the nuclear strangeness radius. For the same reason, the retardation correction to the vector meson pair current operator (Eq. (22c) and Ref. [33]) also does not contribute to $\rho_s[\mathrm{nuc}]$, since this correction is proportional to $\tau F_1^{(s)}(\tau)$. As a result, the low-q behavior of the vector meson contribution to $F^{(s)}_{C0}$ is independent of the choice of approach discussed above. This choice takes on relevance only at larger values of momentum-transfer, where the terms proportional to $\tau F_1^{(s)}(\tau)$ are non-negligible.

III. Calculation of ^{4}He Matrix Elements. Although the object of this paper is to report on a calculation of $F^{T=0}_{C0}$ and $F^{(s)}_{C0}$ using state of the art wavefunctions, we first summarize a simpler calculation of the ^{4}He strangeness radius using a shell model ground state with harmonic oscillator wavefunctions. This simpler treatment allows for an analytical computation and serves to guide one's intuition when interpreting results obtained with more sophisticated methods. The results of the shell model calculation were reported previously [26], and we provide more details in the Appendix of the present paper.

Shell Model Calculation

In the simplest shell model description of ^{4}He, the ground state consists of a single configuration: four nucleons in the $1s_{1/2}$ state. Numerical results using more realistic wavefunctions, such as the variational wavefunction described below, suggest that the level of configuration mixing is at least 15% . Within the S-state approximation, we compute the leading-q behavior of $F^{(s)}_{C0}$ using harmonic oscillator single-particle wavefunctions with an oscillator parameter $b = 1.2$ fm, obtained from fits to the data on $F^{T=0}_{C0}$ [2]. Analytic expressions for the nuclear matrix elements appear in the Appendix, and our results give

$$F^{(s)}_{C0}(\tau\to 0) = \frac{1}{2\sqrt{\pi}}\tau\rho_s[^4\mathrm{He}] \qquad (26)$$

$$= \tau\left(\lambda_1\rho_s+\lambda_{2a}\mu_s+\lambda_{2b}g_{\rho\pi s}\right) \quad ,$$

where the terms containing λ_1 and $\lambda_{2a,b}$ give the one- and two-body contributions, respectively. The one-body term is nuclear structure-independent, since the leading q-dependence of the one-body strangeness Coulomb operator is given by $G_E^{(s)}$ times an operator which counts the number of nucleons (see Eq. (15)). The two-body term $\lambda_{2a}\mu_s$ arises from the vector meson pair currents, while the term $\lambda_{2b}g_{\rho\pi s}$ is generated by the ρ-π transition current. Numerically, in the limit of point meson-nucleon vertices ($\Lambda_M\to\infty$), we obtain $\lambda_1\approx 1.13$, $\lambda_{2a}\approx -0.05$, and $\lambda_{2b}\approx -0.02$ after including a phenomenological NN anti-correlation function in the two-body matrix elements. We expect that the values of the $\lambda_{2a,b}$ for finite Λ_M should be smaller in magnitude than those quoted, which we take to give an upper bound on the scale of two-body contributions. These results imply, then, that $\rho_s[^4\mathrm{He}]$ is at least a factor of 20 more sensitive to the nucleon's strangeness radius than to two-body strangeness currents.

We note in passing that had we not accounted for short range NN repulsion, the vector meson contribution would have been a factor two larger in magnitude and the ρ-π term matrix element would have been a factor of ten larger. The reason for the large suppression of the ρ-π term due to short-range repulsion

can be seen from the structure of the momentum-space ρ-π charge operator in Eq. (24). At leading-order in q, the Coulomb projection of this operator has the form

$$q^2\,\hat{O}\left[\frac{1}{(\vec{k}_1^2+m_\pi^2)(\vec{k}_1^2+m_\rho^2)}\right]+\mathrm{O}(q^4) \qquad (27)$$
$$=\frac{q^2}{(m_\rho^2-m_\pi^2)}\hat{O}\left[\frac{1}{\vec{k}_1^2+m_\pi^2}-\frac{1}{\vec{k}_1^2+m_\rho^2}\right]+\mathrm{O}(q^4)\quad ,$$

where $\hat{O}$ is an operator dependent on $\vec{\sigma}_{1,2}$ and $\vec{k}_1$. Nuclear matrix elements of the full operator in Eq. (27) thus depend on the difference of matrix elements of two operators, $\hat{A}(m_\pi)$ and $\hat{A}(m_\rho)$, whose ranges are set by m_π and m_ρ, respectively. In the absence of short-range anti-correlations, one has $2\langle \mathrm{g.s.}\,\|\hat{A}(m_\pi)\|\,\mathrm{g.s.}\rangle \approx \langle \mathrm{g.s.}\,\|\hat{A}(m_\rho)\|\,g.s.\rangle$. The impact of short range repulsion is to reduce the ρ-meson term $\langle \mathrm{g.s.}\,\|\hat{A}(m_\rho)\|\,g.s.\rangle$ by about a factor of two, while leaving the matrix element of the pionic operator, whose range is much larger than the radius of the repulsive core, relatively unchanged. Consequently, the degree of cancellation between the two pieces is greatly enhanced, leading to the factor of ten reduction in λ_{2b}, as compared with the less significant impact on the magnitude of the purely vector meson matrix elements, λ_{2a}.

Variational Monte Carlo Calculation

The ^{4}He variational wavefunction used in the present work is obtained by minimizing a realistic Hamiltonian with the Argonne v_{14} two-nucleon [41] and Urbana-VIII three-nucleon [42] interaction models. It has the symmetrized product form given by [42]:

$$|\Psi>=\left[1+\sum_{i<j<k}U_{ijk}^{TNI}\right]\left[S\prod_{i<j}(1+U_{ij})\right]|\Psi_J> \quad . \qquad (28)$$

Here S is the symmetrizer, and $|\Psi_J>$ is a Jastrow wavefunction

$$|\Psi_J>=\left[\prod_{i<j}f^c(r_{ij})\right]A|\uparrow p\downarrow p\uparrow n\downarrow n> \ , \qquad (29)$$

where A is the antisymmetrizer acting on the spin-isospin states of the four nucleons. The two-body correlation operator U_{ij} is taken to be

$$U_{ij}=\sum_{p=\tau,\sigma,\sigma\tau,t,t\tau}u^p(r_{ij})O_{ij}^p \qquad (30)$$

with

$$O_{ij}^p=\vec{\tau}_i\cdot\vec{\tau}_j\ ,\ \vec{\sigma}_i\cdot\vec{\sigma}_j\ ,\ \vec{\sigma}_i\cdot\vec{\sigma}_j\vec{\tau}_i\cdot\vec{\tau}_j\ ,\ S_{ij}\ ,\ S_{ij}\vec{\tau}_i\cdot\vec{\tau}_j\ ;\ p=\tau,\sigma,\sigma\tau,t,t\tau\ . \qquad (31)$$

The three-body correlation operator U_{ijk}^{TNI} is simply related to the three-nucleon interaction present in the Hamiltonian, and has a correspondingly complex operator dependence. The correlation functions $f^c(r)$ and $u^p(r)$ as well as the additional parameters present in U_{ijk}^{TNI} are determined variationally with the methods discussed in detail in ref. [42].

The ^{4}He binding energy and charge radius calculated with the above wavefunction have errors of $\simeq 4\%$ when compared to exact Green's Function Monte Carlo (GFMC) results for the same Hamiltonian [42,43] (we note that the GFMC results reproduce the empirical values). This wavefunction also produces a charge form factor that is in good agreement with the exact GFMC predictions and the experimental data over a wide range of momentum transfers [42]. Because of the relatively strong tensor component in the Argonne v_{14} the D-state probability has the rather large value of 16%.

The charge and strangeness form factors are given by the expectation values

$$F_C^{(a)}=2\sqrt{\pi}F_{C0}^{(a)}(q)=<\Psi;\vec{q}\,|\hat{\rho}^{(a)}(\vec{q})|\Psi> \quad , \qquad (32)$$

where $|\Psi;\vec{q}>$ denotes the ground state wavefunction recoiling with momentum $\vec{q}$, and $\hat{\rho}^{(a)}(\vec{q})$ are the r-space representations of the charge and strangeness operators listed in the appendix. The above expectation value is computed, without any approximation, by Monte Carlo integration. The wavefunction is written as a vector in the spin-isospin space of the A-nucleons for any given spatial configuration $\vec{R}\equiv(\vec{r}_1,...,\vec{r}_A)$. For the given $\vec{R}$, we calculate the state vector $\hat{\rho}^{(a)}(\vec{q})|\Psi>$ by performing exactly the spin-isospin algebra with the methods developed in refs. [32,44]. The momentum-dependent terms in $\hat{\rho}^{(a)}$ are calculated numerically; for example,

$$\nabla_{i,\alpha}\Psi(\vec{R})=\frac{1}{2\delta_{i,\alpha}}[\Psi(\vec{R}+\delta_{i,\alpha})-\Psi(\vec{R}-\delta_{i,\alpha})] \ , \qquad (33)$$

where $\delta_{i,\alpha}$ is a small increment in the $r_{i,\alpha}$ component of $\vec{R}$. The $\vec{R}$-integration is carried out with Monte Carlo techniques by sampling a large set of $\vec{R}$ configurations with the Metropolis algorithm.

The two-body pion and ρ-meson operators have been constructed from the Argonne v_{14} following the method outlined in ref. [44]. This implies replacing the propagators in eqs. (22a-c) by the Fourier transforms $v^{\sigma\tau}(k)$ and $v^{t\tau}(k)$ of

the isospin dependent spin-spin and tensor components of the interaction model as

$$\frac{g^2_{\pi NN}}{4m_N^2}\frac{1}{k^2+m_\pi^2} \rightarrow V_\pi(k) = 2v^{t\tau}(k) - v^{\sigma\tau}(k) \tag{34a}$$

$$-\frac{g^2_{\rho NN}(1+\kappa_\rho)^2}{4m_N^2}\frac{1}{k^2+m_\rho^2} \rightarrow V_\rho(k) = v^{t\tau}(k) + v^{\sigma\tau}(k) \tag{34b}$$

The replacements eq.(34) are the ones required for the construction of a two-body electromagnetic current operator that satisfies the continuity equation with the interaction model [44]. We here apply this replacement to the pair current EM and strangeness charge operators as the generalized propagators constructed in this way are then consistent with the short-range behavior of the corresponding interaction components. This short-range behavior is determined phenomenologically by fitting NN elastic scattering data. An additional justification for using the construction eq.(34) is that it has been shown to lead to predictions for the charge and magnetic form factors of the trinucleons [32,42,44], and threshold electrodisintegration of the deuteron [45] that are in reasonably good agreement with the empirical data. The ω-meson propagator in the corresponding pair current, Eqs. (22b,c), and the ρ- and π-meson propagators in the transition current, Eq.(23), are modified by the inclusion of monopole meson-nucleon form factors

$$F_{NNM}(k^2) = \frac{\Lambda_M^2 - m_M^2}{k^2+\Lambda_M^2} \quad , \tag{35}$$

where M is the exchanged meson of mass m_M and Λ_M is a cut-off parameter. We use the values $\Lambda_{NN\omega} = \Lambda_{NN\rho} = \Lambda_{NN\pi} = 2$ GeV, as obtained in boson exchange interaction models [46]. It should be emphasized that the contributions due to the vector meson pair currents are not significant in the momentum transfer range of interest here. Furthermore, we note that in evaluating the contributions due to the vector meson pair currents that include the retardation correction, the non-local terms in eq.(22c), namely those proportional to $\vec{p}+\vec{p}'$, have been neglected. This is justified for the ρ-meson pair current, since the non-local contribution is suppressed by a factor $(1+\kappa_\rho)^2$ ($\kappa_\rho = 6.6$) with respect to the leading term proportional to $F_1^{(s)}(\tau)$. This approximation, however, is questionable for the ω-meson pair current, since in this case the tensor coupling is small, $\kappa_\omega = -0.12$.

IV. Results and Discussion. The results of our VMC calculation are displayed in Figs. 2-6. In computing various contributions to $F_{C0}^{T=0}$ and $F_{C0}^{(s)}$, we have employed a value of $\lambda_E^{(s)} = \lambda_n = 5.6$ to serve as a point of comparison, although $\lambda_E^{(s)}$ is essentially a free parameter characterizing the next-to-leading Q^2-dependence of $G_E^{(s)}$ and is to be constrained by experiment.

Assuming the values $\rho_s = -2.12$ and $\mu_s = -0.2$ for the strangeness radius and magnetic moment of the nucleon, we find that the relativistic Darwin-Foldy and spin-orbit corrections to the single nucleon operator, and the two-body contributions associated with pseudoscalar and vector meson exchanges as well as the $\rho\pi$ transition current lead to about 0.5% decrease (increase in magnitude) of $\rho_s[^4\mathrm{He}]$, a negligible effect.

Results for $F_C^{T=0} = 2\sqrt{\pi}F_{C0}^{T=0}$ and $F_C^{(s)} = 2\sqrt{\pi}F_{C0}^{(s)}$ over a range of momentum-transfer are shown in Figs. 2 and 3. Panels 2(a) and 3(a) give the full form factor resulting from the one- and two-body currents as well as in the impulse approximation (IA) for comparison. Panels 2(b) and 3(b) display individual contributions from the various one- and two-body terms. As indicated by the plot in Fig. 2(a) and as noted in previous work [32], the inclusion of MEC's significantly improves the degree of agreement with the data on $F_C^{T=0}$ over a wide range of q as compared with the IA form factor. The difference in behavior between $F_C^{T=0}$ and $F_C^{(s)}$ at low-q is dictated by the different values of the corresponding nuclear charges: $F_C^{T=0}(0) = AG_E^{T=0}(0) = 2$ and $F_C^{(s)}(0) = AG_E^{(s)}(0) = 0$. At larger values of q, the nuclear EM and strangeness form factors manifest similar structures, having their first diffraction mimina and subsequent maxima at essentially the same values of momentum transfer. Since the various contributions to $F_C^{T=0}(q)$ are discussed elsewhere [32], we focus on $F_C^{(s)}(q)$. At low momentum transfer, the nuclear strangeness form factor is dominated by the single nucleon contribution proportional to $G_E^{(s)}$. In this regime, the largest corrections arise from the spin-orbit and $\rho-\pi$ transition currents. At moderate values of momentum transfer ($q \gtrsim 2$ fm), the largest corrections are due to the pionic pair and $\rho-\pi$ transition currents. In arriving at the results shown in this figure, we have assumed essentially the Jaffe value for the nucleon's strangeness radius ($\rho_s \approx -2$) and a value of $\mu_s = -0.2$. Under this assumption of what would be a large magnitude for ρ_s, the one-body, pionic, and $\rho-\pi$ transition contributions are of the same order of magnitude at the kinematics of the approved CEBAF experiment [24] ($q = 3.93$ fm^{-1}). At this point, the ρ-π contribution makes up about 20% of the total $F_C^{(s)}$. Were we to employ, instead, the results of the kaon-loop estimates of the strangeness parameters, $\rho_s \approx 0.4$ and $\mu_s \approx -0.3$ [20], the magnitude of $F_C^{(s)}$ would be an order of magnitude smaller and would be dominated by the ρ-π contribution.

We emphasize that the relative importance of the pionic operator is highly dependent on one's model for the one-body strangeness form factor, $F_1^{(s)}$, which

enters the two-body operator multiplicatively. In this case, the scale of the two-body operator is set by the Dirac one-body strangeness radius,

$$\rho_s^{\rm Dirac} = \left.\frac{dF_1^{(s)}}{d\tau}\right|_{\tau=0} = \rho_s^{\rm Sachs} + \mu_s \quad . \tag{36}$$

In arriving at the results displayed in Fig. 3, we used essentially the pole model value [16] for $\rho_s^{\rm Dirac} \approx -2.4$, but not the Q^2-dependence for $F_1^{(s)}$, since the latter is un-realistically gentle in light of simple quark counting arguments. Had we used, instead, the results of the kaon loop estimate of Ref. [20], the magnitude of the pionic contribution would have been a factor of 20 smaller than the contribution shown in Fig. 3, and the sign would have been opposite. Similarly, the one-body IA contribution would be reduced by at least a factor of four in magnitude and its sign would also have been opposite than what appears in Fig. 3. In this case, the $\rho - \pi$ transition current would generate the dominant contribution to $F_C^{(s)}$ at the kinematics of the approved CEBAF experiment [24], while the single nucleon strangeness radius would still govern the low-q behavior of the nuclear strangeness form factor.

By way of comparison, we note that the vector meson pair current contribution to $F_C^{(s)}$ is negligible at moderate values of q. Although the precise numerical values of their contributions depend on one's model for $G_M^{(s)}$ and $G_E^{(s)}$, as well as on one's choice as to the treatment of the retardation term, the overall magnitude of the vector meson pair current contribution is sufficiently small so as to render the impact of these model-dependencies negligible.

In Figures 4 and 5, we plot the ratio $R_s = F_{C0}^{(s)}(q)/F_{C0}^{T=0}(q) = F_C^{(s)}(q)/F_C^{T=0}(q)$, which characterizes the s-quark corrections to the non-strange PV asymmetry (Eqs. (3) and (6)). Assuming $|G_E^{(s)}/G_E^n| \approx 1$ and $|G_M^{(s)}/G_M^{T=0}| \approx 1$, which essentially corresponds to assuming the Jaffe values for ρ_s and μ_s but a more realistic momentum-dependence in the strange form factors, we expect a 35% correction to the non-strange asymmetry (the first term on the right side of Eq. (6)) at the kinematics of the CEBAF PV ^{4}He experiment. Fig. 4 shows the dependence of this correction on the value of μ_s which, under our form factor parameterization (Eqs. (12-13)), sets the scale of contributions generated by $G_M^{(s)}$. For purposes of illustration, we have assumed magnitudes and relative signs $G_E^{(s)}/G_E^n \approx -1$ and $G_M^{(s)}/G_E^{T=0} \approx -1$ and have taken a positive sign for $g_{\rho\pi s}$. The results at low-q imply a negligible dependence of $F_{C0}^{(s)}$ on μ_s in this regime. For momentum transfers in the vicinity of those suggested for the approved CEBAF ^{4}He experiment, the ratio changes by $\lesssim 15\%$ as μ_s is varied over a range of values suggested by model calculations [16-21]. Had we assumed the kaon loop values for ρ_s and μ_s, the overall size of the ratio R_s would have been nearly ten times smaller, so that in this case the relative impact of any uncertainty in μ_s would be correspondingly enhanced.

Fig. 5 displays the impact on R_s made by the choice of sign of $g_{\rho\pi s}$, which one cannot determine from ϕ-decay data and symmetry arguments. We illustrate this sensitivity for two different models of nucleon strangeness: (A) $(\rho_s, \mu_s) = (-2.0, -0.2)$ and (B) $(\rho_s, \mu_s) = (0.0, -0.2)$. For low momentum-transfer, the impact of this uncertainty in sign is negligible, whereas at $q \approx 4$ fm^{-1} (the kinematics of Ref. [24]), it corresponds to roughly a $\pm 15\%$ uncertainty in the asymmetry. To put the point somewhat differently, even if the strange quark vector current matrix elements of the nucleon vanished identically, we would expect non-nucleonic strange quarks in the nuclear medium to generate a 15% correction to the non-strange PV asymmetry at the kinematics of Ref. [24]. The scale of this effect is well below the 40% statistical error projected for the approved CEBAF experiment, assuming 50% beam polarization (the error is reduced to 28% for 70% beam polarization). Thus, for a measurement of $A_{LR}(^4\mathrm{He})$ to be sensitive to $g_{\rho\pi}^{(s)}(Q^2)$, significantly a longer running time and/or higher beam polarization would be required.

In Fig. 6, we present the significance of a moderate-q $A_{LR}(^4\mathrm{He})$ measurement from a somewhat different perspective. If one wishes to constrain the various strangeness parameters ρ_s, μ_s, and $\lambda_E^{(s)}$ at a level necessary to test model predictions in detail, then a combination of experiments using proton and $A > 1$ targets would be required [1,2,22]. As noted in Refs. [1,2,22], a combination of low- and moderate-q PV experiments with ^{4}He could potentially constrain $(\rho_s, \lambda_E^{(s)})$ more tightly than could a sequence of $A_{LR}(\vec{e}p)$ measurements alone. This conclusion was based on a one-body (1A) calculation and the ideal assumption of 100% beam polarization with experimental errors being statistics dominated. The inclusion of two-body currents does not alter our previous conclusion about the possible constraints attainable from a low-q measurement, since the two-body contribution is negligible in this regime. In Fig. 6, we display the impact of two-body currents on constraints attainable at moderate-q. Fig. 6a shows the joint constraints on (ρ_s, μ_s) a 10% measurement of $A_{LR}(^4\mathrm{He})$ could produce, assuming the parameterization of Eqs. (12-13) and central values for these parameters given by model (A) discussed above. A similar plot for $(\rho_s, \lambda_E^{(s)})$ constraints is given in Fig. 6b, where a central value for $(\rho_s, \lambda_E^{(s)}) = (-2, \lambda_n)$ is assumed. The solid and dashed lines give the constraints corresponding to different choices as to the sign of $g_{\rho\pi s}$. We take the difference between these two sets of lines as one measure of the theoretical uncertainty associated with our calculation.

From Fig. 6a, we note that the correlation between ρ_s and μ_s is weak. This feature follows from the relatively small magnitudes of the vector meson pair current and spin-orbit contributions, which carry the strongest dependences on μ_s. In the case of Fig. 6b, we observe that the moderate-q constraints are modified only slightly from the IA expectation, even though many-body currents generate significant contributions to $F_{C0}^{(s)}$ and $F_{C0}^{T=0}$. The reason for the insensitivity of these constraints to the two-body currents can be explained in the following manner. First, the pionic corrections are proportional to the Dirac form factor

$$F_1^{(a)} = (1+\tau)^{-1}\left[G_E^{(a)} + \tau G_M^{(a)}\right] \quad , \tag{37}$$

where "a" denotes either the isoscalar EM current or strange quark current. At the kinematics of the moderate-q CEBAF PV experiment, one has $\tau \approx 0.17$ so that $\tau G_M^{T=0}/G_E^{T=0} \approx 0.15$. In this case, $F_1^{T=0} \approx G_E^{T=0}$. Similarly, $\tau G_M^{(s)}/G_E^{(s)} \approx \mu_s/\rho_s \approx 0.15$, assuming the Jaffe values for the strangeness parameters, so that $F_1^{(s)} \approx G_E^{(s)}$. Under these assumptions, the pionic pair currents give the dominant correction to the IA nuclear form factors, so that at $\tau = 0.17$ ($q^2 = 0.6\,(\mathrm{GeV}/c)^2$) one has

$$\begin{aligned} F_{C0}^{T=0}(q) &\approx \langle \text{g.s.} \,\|\hat{M}_0^{T=0}(q)^{[1]} + \hat{M}_0^{T=0}(q)^{[2]}_{\text{pionic}}\|\, \text{g.s.}\rangle \\ &\approx G_E^{T=0}(\tau)\langle \text{g.s.} \,\|\hat{\mathcal{O}}(q)^{[1]} + \hat{\mathcal{O}}(q)^{[2]}\|\, \text{g.s.}\rangle \end{aligned} \tag{38a}$$

$$\begin{aligned} F_{C0}^{(s)}(q) &\approx \langle \text{g.s.} \,\|\hat{M}_0^{(s)}(q)^{[1]} + \hat{M}_0^{(s)}(q)^{[2]}_{\text{pionic}}\|\, \text{g.s.}\rangle \\ &\approx G_E^{(s)}(\tau)\langle \text{g.s.} \,\|\hat{\mathcal{O}}(q)^{[1]} + \hat{\mathcal{O}}(q)^{[2]}\|\, \text{g.s.}\rangle \quad , \end{aligned} \tag{38b}$$

where $\hat{\mathcal{O}}(q)^{[1]}$ and $\hat{\mathcal{O}}(q)^{[2]}$ are nuclear operators (see, *e.g.*, Eqs. (15) and (A.1)). Hence, the ratio $R_s = F_{C0}^{(s)}/F_{C0}^{T=0}$ is essentially independent of nuclear matrix elements and is governed by the ratio of single nucleon form factors as in the IA case. Thus, the inclusion of two-body currents does not seriously change the joint constraints on ρ_s and $\lambda_E^{(s)}$. Some changes from the IA results do appear, since neither $G_M^{(s)}$ nor the ρ-π constributions are completely negligible. In the event that $|\mu_s/\rho_s| >> 0.15$, however, this argument would break down and our conclusions would have to be modified.

We also point out that the uncertainty in the sign of the ρ-π transition current contribution does not seriously affect the $(\rho_s, \lambda_E^{(s)})$ constraints, even though the magnitude of this contribution is as large as the experimental uncertainty in A_{LR} assumed in obtaining the plots of Fig. 6. To understand why this is the case, consider the following argument. If one assumes that all of δA_{LR} translates into an uncertainty δR_s in the extracted value of R_s, and if one further assumes that ρ_s and $\lambda_E^{(s)}$ can be varied in a manner consistent with this uncertainty δR_s (as we've done in obtaining the lines in Fig. 6b), then one has

$$\frac{\delta A_{LR}}{A_{LR}} = \frac{\delta R_s}{4\sin^2\theta_W + R_s} \tag{38}$$

or

$$\delta R_s = (4\sin^2\theta_W + R_s)\,\frac{\delta A_{LR}}{A_{LR}} \approx 0.1 + 0.1\,R_s \tag{40}$$

for $\delta A_{LR}/A_{LR} = 0.1$. Since R_s changes by only ± 0.1 for different choices for the sign of $g_{\rho\pi s}$, the impact of this choice on the magnitude of δR_s – and, therefore on the joint constraints on $(\rho_s, \lambda_E^{(s)})$ – is an order of magnitude smaller than the impact of the experimental error in A_{LR}.

Finally, in Fig. 7 we show the ρ-meson pair current contribution to $F_C^{(s)}$ under the two different assumptions as to the inclusion of the retardation correction. The curve labelled by "$\rho_\#$" was calculated without the retardation correction (Gari-Hyuga convention [36]), while the curve labelled by "ρ" includes it (Riska convention [32,33]). The difference between the two should be taken as an estimate of the theoretical uncertainty in the treatment of these short-range currents. Fortunately, the scale of the vector meson contributions is sufficiently small that the choice of convention has a negligible impact on the value of $F_C^{(s)}$.

V. Conclusions. We have computed MEC contributions to the ^{4}He strange quark elastic form factor, $F_C^{(s)} = 2\sqrt{\pi}F_{C0}^{(s)}(q)$, using Monte Carlo methods and an accurate variational ground state wavefunction. Our results indicate that the nuclear strangeness radius, ρ_s[nuc], which governs $F_C^{(s)}(q)$ at low momentum-transfer, is (1) dominated by the single nucleon strangeness radius, (2) two orders of magnitude less sensitive to many-body strangeness currents, and (3) independent of pionic MEC's – results which essentially confirm our previous conclusions based on the shell model calculation. At moderate values of q, such as those corresponding to the approved CEBAF elastic PV ^{4}He experiment [24], we find that $F_C^{(s)}$ generates a 35% correction to the PV asymmetry, assuming that $|G_E^{(s)}/G_E^n| \approx 1$ and $|G_M^{(s)}/G_M^{T=0}| \approx 1$ in this regime and that $g_{\rho\pi}^{(s)}(Q^2)$ is correctly given by ϕ-meson dominance. The magnitude of this correction is smaller than the statistical error projected for the CEBAF experiment under the most conservative assumptions about beam polarization. In the absence of nucleonic strangeness, non-nucleonic $s\bar{s}$ pairs would generate roughly a 15% correction to

the non-strange asymmetry at these kinematics. Thus, the scale of the strange-quark contribution to $A_{LR}(^4\mathrm{He})$ is still sensitive to the nucleon's strangeness electric form factor. In the event that $|G_E^{(s)}/G_E^n| << 1$, a more precise ^{4}He PV measurement could probe the ρ-π strangeness charge operator. Such a measurement would be interesting since only a ρ-π transition three-current operator has been probed in other experiments performed to date [27]. Finally, inclusion of MEC contributions to $F_C^{(s)}$ and $F_C^{T=0}$ does not appear to affect noticeably the constraints on the leading and next-to-leading Q^2-dependence of $G_E^{(s)}$ attainable with a medium-q measurement of the ^{4}He PV asymmetry.

Acknowledgements

We thank R.B. Wiringa for making available to us the latest version of his variational ^{4}He wavefunction. We also thank J. Goity, E.J. Beise and D.O. Riska for useful discussions.

APPENDIX

In this Appendix, we provide complete expressions for the two-body charge operators, expressions for the low-q forms of the corresponding Coulomb projections, and additional details of our shell model calculation of the nuclear strangeness radius.

Two-body charge operators

Expressions for the co-ordinate space charge operators can be obtained by Fourier-transforming the momentum-space operators in Eq. (22) and (24) and summing over all nucleon pairs. The resulting formulae are

$$\hat{\rho}(\vec{q})^{[2]}_{\mathrm{pionic}} = -i\left[\frac{g_{\pi NN}^2}{16\pi m_N^3}\right] F_1^{(a)}(\tau)\sum_{i<j}\delta(\vec{x}_i-\vec{x}_i')\delta(\vec{x}_j-\vec{x}_j')\vec{\tau}_i\cdot\vec{\tau}_j \qquad \text{(A.1)}$$
$$\times\left[\frac{\mathrm{e}^{-m_\pi r_{ij}}}{r_{ij}^2}\right](1+m_\pi r_{ij})\left[\mathrm{e}^{i\vec{q}\cdot\vec{x}_i}\sigma_i\cdot\vec{q}\vec{\sigma}_j\cdot\hat{r}_{ij}-\mathrm{e}^{i\vec{q}\cdot\vec{x}_j}\vec{\sigma}_j\cdot\vec{q}\vec{\sigma}_i\cdot\hat{r}_{ij}\right]$$

for the pionic current,

$$\hat{\rho}(\vec{q})^{[2]\ (a)}_{\mathrm{V-pair}} = \left[\frac{g_{VNN}^2}{16\pi m_N^3}\right] G_M^{(a)}(\tau)\sum_{i<j}\hat{T}_V(i,j)\delta(\vec{x}_i-\vec{x}_i')\delta(\vec{x}_j-\vec{x}_j') \qquad \text{(A.2a)}$$
$$\left\{\left[\frac{\mathrm{e}^{-m_V r_{ij}}}{r_{ij}}\right]\left[\mathrm{e}^{i\vec{q}\cdot\vec{x}_j}(\vec{\sigma}_i\times\vec{q})\cdot\vec{\nabla}_j+\mathrm{e}^{i\vec{q}\cdot\vec{x}_i}(\vec{\sigma}_j\times\vec{q})\cdot\vec{\nabla}_i\right]\right.$$
$$\left.+i(1+\kappa_V)\left[\frac{\mathrm{e}^{-m_V r_{ij}}}{r_{ij}^2}\right](1+m_V r_{ij})\left[\mathrm{e}^{i\vec{q}\cdot\vec{x}_j}(\vec{q}\cdot\hat{r}_{ij}+\vec{\sigma}_j\times\vec{q}\cdot\vec{\sigma}_i\times\hat{r}_{ij})\right.\right.$$
$$\left.\left.-\mathrm{e}^{i\vec{q}\cdot\vec{x}_i}(\vec{q}\cdot\hat{r}_{ij}+\vec{\sigma}_i\times\vec{q}\cdot\vec{\sigma}_j\times\hat{r}_{ij})\right]\right\}$$

for the vector meson pair current in the absence of the retardation term and

$$\hat{\rho}(\vec{q})^{[2]\ (b)}_{\mathrm{V-pair}} = \hat{\rho}(\vec{q})^{[2]\ (a)}_{\mathrm{V-pair}} + i\kappa_V(1+\kappa_V)\left[\frac{g_{VNN}^2}{16\pi m_N^3}\right]F_1^{(a)}(\tau) \qquad \text{(A.2b)}$$
$$\times\sum_{i<j}\hat{T}(i,j)\delta(\vec{x}_i-\vec{x}_i')\delta(\vec{x}_j-\vec{x}_j')\left[\frac{\mathrm{e}^{-m_V r_{ij}}}{r_{ij}^2}\right](1+m_V r_{ij})$$
$$\times\left[\mathrm{e}^{i\vec{q}\cdot\vec{x}_j}\vec{\sigma}_j\times\vec{q}\cdot\vec{\sigma}_i\times\hat{r}_{ij}-\mathrm{e}^{i\vec{q}\cdot\vec{x}_i}\vec{\sigma}_i\times\vec{q}\cdot\vec{\sigma}_j\times\hat{r}_{ij}\right]$$

with the retardation term included. The ρ-π transition current operator is given by

$$\hat{\rho}(\vec{q})^{[2]}_{\rho\pi} = -\left[\frac{g_{\pi NN}g_{VNN}g_{\rho\pi}^{(a)}(\tau)}{32\pi m_N^2 m_\rho}\right]\sum_{i<j}\delta(\vec{x}_i-\vec{x}_i')\delta(\vec{x}_j-\vec{x}_j')\vec{\tau}_i\cdot\vec{\tau}_j\mathrm{e}^{i\vec{q}\cdot\vec{R}_{ij}}\Gamma(i,j) \qquad \text{(A.3)}$$

where

$$\Gamma(i,j) = i\left[F_1(\vec{r}_{ij})\overleftrightarrow{\nabla}_j\cdot(\hat{r}_{ij}\times\vec{q})\vec{\sigma}_i\cdot\vec{q}-F_1(-\vec{r}_{ij})\overleftrightarrow{\nabla}_i\cdot(\hat{r}_{ij}\times\vec{q})\vec{\sigma}_j\cdot\vec{q}\right] \qquad \text{(A.4)}$$
$$+F_2(\vec{r}_{ij})\overleftrightarrow{\nabla}_j\cdot(\hat{r}_{ij}\times\vec{q})\hat{r}_{ij}\cdot\vec{\sigma}_i+F_2(-\vec{r}_{ij})\overleftrightarrow{\nabla}_i\cdot(\hat{r}_{ij}\times\vec{q})\hat{r}_{ij}\cdot\vec{\sigma}_j$$
$$+F_3(\vec{r}_{ij})\overleftrightarrow{\nabla}_j\cdot(\vec{\sigma}_i\times\vec{q})+F_3(-\vec{r}_{ij})\overleftrightarrow{\nabla}_i\cdot(\vec{\sigma}_j\times\vec{q})$$
$$+(1+\kappa_\rho)\left\{\vec{\sigma}_i\cdot\vec{\sigma}_j\left[i\left\{G_1(\vec{r}_{ij})+G_1(-\vec{r}_{ij})\right\}+\vec{q}\cdot\hat{r}_{ij}\left\{H_1(\vec{r}_{ij})-H_1(-\vec{r}_{ij})\right\}\right]\right.$$
$$+\vec{q}\cdot\vec{\sigma}_i\vec{q}\cdot\vec{\sigma}_j\left[i\left\{G_2(\vec{r}_{ij})+G_2(-\vec{r}_{ij})\right\}+\vec{q}\cdot\hat{r}_{ij}\left\{H_2(\vec{r}_{ij})-H_2(-\vec{r}_{ij})\right\}\right]$$
$$+\hat{r}_{ij}\cdot\vec{\sigma}_i\hat{r}_{ij}\cdot\vec{\sigma}_j\left[i\left\{G_3(\vec{r}_{ij})+G_3(-\vec{r}_{ij})\right\}+\vec{q}\cdot\hat{r}_{ij}\left\{H_3(\vec{r}_{ij})-H_3(-\vec{r}_{ij})\right\}\right]$$
$$+\hat{r}_{ij}\cdot\vec{\sigma}_i\vec{q}\cdot\vec{\sigma}_j\left[\left\{G_4(\vec{r}_{ij})-G_5(-\vec{r}_{ij})\right\}+i\vec{q}\cdot\hat{r}_{ij}\left\{H_4(\vec{r}_{ij})+H_5(-\vec{r}_{ij})\right\}\right]$$
$$\left.+\hat{r}_{ij}\cdot\vec{\sigma}_j\vec{q}\cdot\vec{\sigma}_i\left[\left\{G_5(\vec{r}_{ij})-G_4(-\vec{r}_{ij})\right\}+i\vec{q}\cdot\hat{r}_{ij}\left\{H_5(\vec{r}_{ij})+H_4(-\vec{r}_{ij})\right\}\right]\right\}$$

where

$$F_1(\vec{r}) = -\left(g_1+\frac{g_0}{2}\right) \qquad \text{(A.5a)}$$

$$F_2(\vec{r}) = h_0 + \frac{g_0}{r}$$
$$F_3(\vec{r}) = -\frac{g_0}{r}$$

$$G_1(\vec{r}) = -\frac{1}{r}\left(g_1 - \frac{g_0}{2}\right) q^2 \qquad \text{(A.5b)}$$
$$G_2(\vec{r}) = \frac{2g_1}{r} - h_1 - \frac{h_0}{2}$$
$$G_3(\vec{r}) = q^2\left[\frac{1}{r}\left(g_1 - \frac{g_0}{2}\right) + \left(h_1 - \frac{h_0}{2}\right)\right]$$
$$G_4(\vec{r}) = k_0 - \frac{h_0}{r}$$
$$G_5(\vec{r}) = \frac{h_0}{r} + q^2\left(g_2 - \frac{g_0}{4}\right)$$

$$H_1(\vec{r}) = \frac{1}{r}\left(h_0 + \frac{g_0}{r}\right) \qquad \text{(A.5c)}$$
$$H_2(\vec{r}) = \frac{g_0}{4} - g_2$$
$$H_3(\vec{r}) = -\left(k_0 + \frac{3h_0}{r} + \frac{3g_0}{r^2}\right)$$
$$H_4(\vec{r}) = -\left[\left(h_1 - \frac{h_0}{2}\right) + \frac{1}{r}\left(g_1 - \frac{g_0}{2}\right)\right]$$
$$H_5(\vec{r}) = \frac{1}{r}\left(g_1 + \frac{g_0}{2}\right) + \left(h_1 + \frac{h_0}{2}\right)$$

and where

$$g_n(\vec{r},\vec{q}) = \int_{-1/2}^{1/2} d\beta\beta^n \exp\left[i\beta\vec{q}\cdot\vec{r} - Lr\right] \qquad \text{(A.6)}$$

$$h_n(\vec{r},\vec{q}) = \int_{-1/2}^{1/2} d\beta\beta^n \; L \; \exp\left[i\beta\vec{q}\cdot\vec{r} - Lr\right]$$

$$k_n(\vec{r},\vec{q}) = \int_{-1/2}^{1/2} d\beta\beta^n \; L^2 \; \exp\left[i\beta\vec{q}\cdot\vec{r} - Lr\right]$$

with

$$L^2 = \frac{1}{2}(m_\pi^2 + m_\rho^2) + \beta(m_\rho^2 - m_\pi^2) + (1/4 - \beta^2)q^2 \qquad \text{(A.7)}$$

We define

$$\overleftrightarrow{\nabla}_i = \overleftarrow{\nabla}_i - \overrightarrow{\nabla}_i \quad , \qquad \text{(A.8)}$$

where $\overleftarrow{\nabla}_i$ and $\overrightarrow{\nabla}_i$ are gradients acting to the left and right, respectively, on the co-ordinate of the i-th nucleon in the wavefunction (and not on the co-ordinates appearing in the operators). The isospin tensor $T_V(i,j)$ is defined in Eq. (23), the quantities $\vec{x}_i$ and $\vec{x}_i'$ are the co-ordinate of the i-th nucleon in the initial and final state wavefunction, respectively, and where the co-ordinates $\vec{r}_{ij}$ *etc.* are defined in Eq. (A.11) below. As elsewhere, the superscript "a" denotes either the $T = 0$ EM current or strangeness current operators.

Expressions for the pair current operators with hadronic form factors included (finite Λ_M) may be obtained from the above formulae by making the replacement

$$\hat{O}(m_M) \to \hat{O}(m_M) - \hat{O}(\Lambda_M) + \frac{(\Lambda_M^2 - m_M^2)}{2\Lambda_M}\frac{d}{d\Lambda_M}\hat{O}(\Lambda_M) \quad , \qquad \text{(A.9)}$$

where $\hat{O}(m_M)$ is any one of the pair current operators in Eqs. (A.1,2) associated with the exchange of a meson having mass m_M. Similarly, for the ρ-π transition current, the Coulomb operator in the presence of hadronic form factors arises from making the replacement

$$\hat{O}(m_\pi, m_\rho) \to \hat{O}(m_\pi, m_\rho) + \hat{O}(\Lambda_\pi, \Lambda_\rho) - \hat{O}(m_\pi, \Lambda_\rho) - \hat{O}(\Lambda_\pi, m_\rho) \quad , \qquad \text{(A.10)}$$

where $\hat{O}(m_\pi, m_\rho)$ is the operator appearing in Eq. (A.3).

Substituting the above expressions for the charge operators into Eq. (7c) and expanding the exponentials in powers of $\vec{q}$ leads to the following expressions for the leading q-dependence of the Coulomb operators:

$$\hat{M}_{00}^{[2]}(q)\Big|_{q\to 0}^{\text{pionic}} = \tau\left[\frac{g_{\pi NN}^2}{24\pi^{3/2}m_N}\right] F_1^{(a)}(\tau)\sum_{i<j}\delta(\vec{x}_i - \vec{x}_i')\delta(\vec{x}_j - \vec{x}_j')\vec{\tau}_i\cdot\vec{\tau}_j \qquad \text{(A.10a)}$$
$$\times\left[\frac{e^{-m_\pi r_{ij}}}{m_\pi r_{ij}}\right](1 + m_\pi r_{ij})\left[\frac{1}{3}\vec{\sigma}_i\cdot\vec{\sigma}_j\right.$$
$$\left.+\sqrt{\frac{8\pi}{3}}[Y_2(\hat{r}_{ij})\otimes[\sigma_i\otimes\sigma_j]_2]_0 + \left(\frac{R_{ij}}{r_{ij}}\right)(\hat{R}_{ij}\times\hat{r}_{ij})\cdot(\vec{\sigma}_i\times\vec{\sigma}_j)\right] \quad ,$$

$$\hat{M}^{[2]}_{00}(q)\Big|^{V-\mathrm{pair}}_{q\to 0} = \tau G^{(a)}_M(\tau)\left[\frac{g^2_{VNN}m_V}{24\pi^{3/2}m_N}\right]\sum_{i<j}\delta(\vec{x}_i-\vec{x}_i')\delta(\vec{x}_j-\vec{x}_j')\hat{T}_V(i,j)$$

(A.10b)

$$\times\left[\frac{\mathrm{e}^{-m_V r_{ij}}}{m_V r_{ij}}\right]\Bigg\{(1+\kappa_V)(1+m_V r_{ij})\Bigg[1+\frac{2}{3}\vec{\sigma}_i\cdot\vec{\sigma}_j$$

$$-\sqrt{\frac{8\pi}{3}}\,[Y_2(\hat{r}_{ij})\otimes[\sigma_i\otimes\sigma_j]_2]_0$$

$$+\left(\frac{R_{ij}}{r_{ij}}\right)(\hat{r}_{ij}\times\hat{R}_{ij})\cdot(\vec{\sigma}_i\times\vec{\sigma}_j)\Bigg]+\vec{\Sigma}_{ij}\cdot(\vec{L}^{ij}_R-2\vec{L}^{ij}_r)$$

$$-i\vec{\Delta}_{ij}\cdot(\hat{r}_{ij}\times\vec{\nabla}_{R_{ij}}-2\hat{R}_{ij}\times\vec{\nabla}_{r_{ij}})$$

$$-i\left(\frac{R_{ij}}{r_{ij}}\right)(1+m_V r_{ij})\vec{\Delta}_{ij}\cdot(\hat{R}_{ij}\times\hat{r}_{ij})\Bigg\}\quad ,$$

$$\hat{M}^{[2]}_{00}(q)\Big|^{\rho\pi}_{q\to 0} =$$

$$\tau g^{(a)}_{\rho\pi}(\tau)\left[\frac{g_{\pi NN}g_{\rho NN}}{24\pi^{3/2}}\right]\sum_{i<j}\delta(\vec{x}_i-\vec{x}_i')\delta(\vec{x}_j-\vec{x}_j')\vec{\tau}_i\cdot\vec{\tau}_j$$

(A.10c)

$$\times\frac{1}{m_\rho r_{ij}}\left[\frac{1}{(m_\rho r_{ij})^2-(m_\pi r_{ij})^2}\right]\Bigg\{(1+\kappa_\rho)\Bigg[Z_1(i,j)\vec{\sigma}_i\cdot\vec{\sigma}_j$$

$$-\sqrt{\frac{8\pi}{3}}Z_2(i,j)[Y_2(\hat{r}_{ij})\otimes[\sigma_i\otimes\sigma_j]_2]_0$$

$$+\left(\frac{R_{ij}}{r_{ij}}\right)Z_3(i,j)(\hat{r}_{ij}\times\hat{R}_{ij})\cdot(\vec{\sigma}_i\times\vec{\sigma}_j)\Bigg]-\frac{1}{2}r_{ij}Z_4(i,j)\vec{\Delta}_{ij}\cdot(\hat{r}_{ij}\times\vec{\nabla}_{R_{ij}})$$

$$+iZ_4(i,j)\vec{\Sigma}_{ij}\cdot(\vec{L}^{ij}_r+\vec{L}^{ij}_R)-2R_{ij}Z_4(i,j)\vec{\Delta}_{ij}\cdot(\hat{R}_{ij}\times\vec{\nabla}_{r_{ij}})$$

$$-2i\left(\frac{R_{ij}}{r_{ij}}\right)Z_2(i,j)\hat{r}_{ij}\cdot\vec{\Delta}_{ij}\hat{R}_{ij}\cdot\vec{L}^{ij}_r-iZ_2(i,j)\vec{\Sigma}_{ij}\cdot\hat{r}_{ij}\hat{r}_{ij}\cdot\vec{L}^{ij}_R\Bigg\}\quad ,$$

where

$$\begin{aligned}\vec{r}_{ij} &= \vec{x}_i-\vec{x}_j\\ r_{ij} &= |\vec{r}_{ij}|\\ \hat{r}_{ij} &= \vec{r}_{ij}/r_{ij}\end{aligned}\qquad\text{(A.11a)}$$

$$\begin{aligned}\vec{R}_{ij} &= \frac{1}{2}(\vec{x}_i+\vec{x}_j)\\ R_{ij} &= |\vec{R}_{ij}|\end{aligned}\qquad\text{(A.11b)}$$

$$\begin{aligned}\vec{L}^{ij}_r &= -i\vec{r}_{ij}\times\vec{\nabla}_{r_{ij}}\\ \vec{L}^{ij}_R &= -i\vec{R}_{ij}\times\vec{\nabla}_{R_{ij}}\end{aligned}\qquad\text{(A.11c)}$$

$$\begin{aligned}\vec{\Sigma}_{ij} &= \vec{\sigma}_i+\vec{\sigma}_j\\ \vec{\Delta}_{ij} &= \vec{\sigma}_i-\vec{\sigma}_j\quad ,\end{aligned}\qquad\text{(A.11d)}$$

and where

$$Z_1(i,j) = (m_\pi r_{ij})^2\mathrm{e}^{-m_\pi r_{ij}}-(m_\rho r_{ij})^2\mathrm{e}^{-m_\rho r_{ij}}\qquad\text{(A.12a)}$$

$$\begin{aligned}Z_2(i,j) = {}&\left[3+3(m_\rho r_{ij})+(m_\rho r_{ij})^2\right]\mathrm{e}^{-m_\rho r_{ij}}\\ &-\left[3+3(m_\pi r_{ij})+(m_\pi r_{ij})^2\right]\mathrm{e}^{-m_\pi r_{ij}}\end{aligned}\qquad\text{(A.12b)}$$

$$\begin{aligned}Z_3(i,j) = {}&\left[2+2(m_\rho r_{ij})+(m_\rho r_{ij})^2+(m_\rho r_{ij})^3\right]\mathrm{e}^{-m_\rho r_{ij}}\\ &-\left[2+2(m_\pi r_{ij})+(m_\pi r_{ij})^2+(m_\pi r_{ij})^3\right]\mathrm{e}^{-m_\rho r_{ij}}\end{aligned}\qquad\text{(A.12c)}$$

$$Z_4(i,j) = [1+m_\rho r_{ij}]\mathrm{e}^{-m_\rho r_{ij}}-[1+m_\pi r_{ij}]\mathrm{e}^{-m_\pi r_{ij}}\quad .\qquad\text{(A.12d)}$$

We note in passing that the overall normalization of the $\rho-\pi$ operator appearing in Eq. (A.10c) differs by a factor of four from that appearing in Eq. (7) of Ref. [26]. The latter, as well as the terms involving $g^{(s)}_{\rho\pi}$ in Eqs. (10) and (14) of that work, should be multiplied by 1/4.

Shell Model Calculation

Use of a simple shell model ^{4}He ground state allows one to obtain analytic expressions for the nuclear strangeneness radius, ρ_s[nuc], which are useful in the interpretation of the numerical results obtained with variational ground state

wavefunctions. To that end, we compute matrix elements of the one- and two-body Coulomb operators in the low-q limit. From the expressions in Eqs. (A.10) and as noted in the main text of the paper, the vector meson pair current and ρ-π transition current Coulomb operators go as q^2 for low-q. The two-body pionic operator, in contrast, vanishes as q^4 since $F_1^{(s)} \sim q^2$ and since the operator carries an additional, explicit factor of q^2. Similarly, the vector meson pair current retardation term also enters at $\mathcal{O}(q^4)$. Thus, for purposes of computing two-body contributions to ρ_s[nuc], we need only compute matrix elements of the operators in Eqs. (A.10b,c). In the limit that the ^{4}He ground state is a pure S-state, the leading q^2-dependence of the one-body matrix element (Eq. (15)) is given by the one-body form factor times the number of nucleons and is independent of details of the nuclear wavefunction. The two-body matrix elements, on the other hand, are structure-dependent. An important consideration in this respect is the short-range repulsion between nucleons. Since the ranges of the ρ- and ω-mesons are commensurate with the radius of the repulsive core in the N-N potential, matrix elements of the vector meson exchange operators ought to be suppressed. To account for this effect, we compute the two-body shell model matrix elements by including a phenomenological correlation function, $g(r)$, in the integral over relative co-ordinates:

$$\int_0^\infty r^2 dr\; u^*(r)\hat{\mathcal{O}}u(r) \to \int_0^\infty r^2 dr\; g(r)\; u^*(r)\hat{\mathcal{O}}u(r) \quad , \tag{A.13}$$

where $u(r)$ is the radial wavefunction for the relative motion of two nucleons, $r = |\vec{x}_1 - \vec{x}_2|$ is the relative co-ordinate, and $\hat{\mathcal{O}}$ is an r-dependent two-body operator. Following the approach of Ref. [34], we take the correlation function to have the form

$$g(r) = C\left[1 - \mathrm{e}^{-r^2/d^2}\right] \quad , \tag{A.14}$$

where the constant C is determined by the requirement that the wavefunction be normalized. A fit to the nuclear matter correlation function of Ref. [47] gives $d = 0.84$ fm. With this form for $g(r)$, the un-correlated two-body matrix elements are modified as

$$\mathrm{M}(b) \to C\left[\mathrm{M}(b) - \mathrm{M}(b_{\mathrm{eff}})\right] \quad , \tag{A.15}$$

where $\mathrm{M}(b)$ is the un-correlated two-body matrix element computed using an oscillator parameter b, where the effective oscillator parameter is given by

$$\left(\frac{b_{\mathrm{eff}}}{b}\right) = \left[1 + 2\left(\frac{b}{d}\right)\right]^{-1/2} \quad , \tag{A.16}$$

and where

$$C = \left[1 - \left(\frac{b_{\mathrm{eff}}}{b}\right)^3\right]^{-1} \quad . \tag{A.17}$$

In the limit of no short-range repulsion ($b_{\mathrm{eff}} \to 0$), one has for the leading q-dependence of $F_{C0}^{(s)}$ the expression given in Eq. (26). The nuclear $\lambda_{1,2}$ are given by

$$\lambda_1 = 2/\sqrt{\pi} \quad , \tag{A.18a}$$

$$\lambda_{2a} = -\sum_{V=\rho,\omega}(1+\kappa_V)\left(\frac{\sqrt{2}g_{VNN}^2}{24\pi^2}\right)\left(\frac{m_V}{m_N}\right)\frac{\mathcal{N}_V}{(m_V b)} \tag{A.18b}$$
$$\times\left\{1 - (m_V b)^2 + \sqrt{\pi/2}(m_V b)^3 \exp\left[\tfrac{1}{2}(m_V b)^2\right]\mathrm{erfc}\left(\frac{m_V b}{\sqrt{2}}\right)\right\}$$
$$\to -\sum_{V=\rho,\omega}(1+\kappa_V)\left(\frac{\sqrt{2}g_{VNN}^2}{8\pi^2}\right)\left(\frac{m_V}{m_N}\right)\frac{\mathcal{N}_V}{(m_V b)^3}\left[1 - \frac{5}{(m_V b)^2} + \cdots\right] \quad ,$$

$$\lambda_{2b} = (1+\kappa_\rho)\left(\frac{\sqrt{2}g_{\pi NN}g_{\rho NN}}{18\pi^2}\right)\frac{\mathcal{N}_2}{(m_\rho b)}\left[\frac{1}{(m_\rho b)^2 - (m_\pi b)^2}\right] \tag{A.18c}$$
$$\times\left[(m_\pi b)^2 I(m_\pi b) - (m_\rho b)^2 I(m_\rho b)\right] \quad ,$$

where

$$I(mb) = 1 - \sqrt{\frac{\pi}{2}}(mb)\exp[\tfrac{1}{2}(mb)^2]\mathrm{erfc}\left(\frac{mb}{\sqrt{2}}\right) \quad , \tag{A.19}$$

and where $\mathcal{N}_{V,2}$ are spin-isospin matrix elements and g_{VNN} is the vector meson-nucleon coupling. For $b = 1.2$ fm, one has $m_\rho b >> 1$, so that the function in Eq. (A.18c) may be expanded as

$$(m_\rho b)^2 I(m_\rho b) = 1 - \frac{3}{(m_\rho b)^2} + \cdots \quad . \tag{A.20}$$

A similar expansion in powers of $1/(m_V b)$ has been used in arriving at the expression in Eq. (A.18b), where the $+\cdots$ indicates contributions from terms higher order in $1/(m_V b)$.

References

1. M. J. Musolf *et al.*, *Physics Reports* **239/1&2** (1994).

2. M. J. Musolf and T.W. Donnelly, *Nucl. Phys.* **A546** (1992) 509; *Nucl. Phys.* **A550** (1992) 564 (E).

3. W. M. Alberico *et al.*, *Nucl. Phys.* **A569** (1994) 701.

4. T. W. Donnelly *et al.*, *Nucl. Phys.* **A541** (1992) 525.

5. D. H. Beck, *Phys. Rev.* **D39** (1989) 3248.

6. MIT-Bates proposal # 89-06, R. D. McKeown and D. H. Beck, contact people.

7. D. B. Kaplan and A. Manohar, *Nucl. Phys.* **B310** (1988) 527.

8. T. P. Cheng, *Phys. Rev.* **D13** (1976) 2161.

9. J. Gasser, H. Leutwyler, and M. E. Sainio, *Phys. Lett.* **B253** (1991) 252.

10. L.A. Ahrens *et al.*, *Phys. Rev.* **D35** (1987) 785.

11. G. Garvey *et al.*, *Phys. Rev.* **C48** (1993) 1919.

12. C. J. Horowitz *et al.*, *Phys. Rev.* **C48** (1993) 3078.

13. J. Ashman *et al.*, *Nucl. Phys.* **B328** (1989) 1.

14. P. L. Anthony *et al.*, *Phys. Lett.* **B302** (1993) 553.

15. B. Adeva *et al.*, *Phys. Rev. Lett.* **71** (1993) 959.

16. R. L. Jaffe, *Phys. Lett.* **B229** (1989) 275.

17. N. W. Park, J. Schechter and H. Weigel, *Phys. Rev.* **D43**, 869 (1991).

18. B. R. Holstein in *Proceedings of the Caltech Workshop on Parity Violation in Electron Scattering*, E.J. Beise and R.D. McKeown, Eds., World Scientific (1990) pp. 27-43.

19. W. Koepf, E.M. Henley, and S.J. Pollock, *Phys. Lett.* **B288** (1992) 11.

20. M. J. Musolf and M. Burkardt, *Z. für Phys.* **C61** (1994) 433.

21. T. Cohen, H. Forkel, and M. Nielsen, *Phys. Lett.* **B316** (1993) 1.

22. M. J. Musolf and T. W. Donnelly, *Z. für Phys.* **C57** (1993) 559.

23. J.D. Walecka in *Muon Physics*, Vol. II, V.W. Hughes and C.S. Wu, Eds., Academic Press (1975) 113.

24. CEBAF proposal # PR-91-004, E.J. Beise, spokesperson.

25. CEBAF proposal # PR-91-017, D.H. Beck, spokesperson.

26. M. J. Musolf and T. W. Donnelly, *Phys. Lett.* **B318** (1993) 263.

27. E. Hummel and J.A. Tjon, *Phys. Rev. Lett* **63** (1989) 1788.

28. R.G. Sachs, *Phys. Rev.* **126** (1962) 2256.

29. T. de Forest, Jr. and J. D. Walecka, *Adv. in Phys.* **15**, (1966) 1.

30. J. D. Bjorken and S. D. Drell, *Relativistic Quantum Mechanics*, McGraw-Hill (New York, 1964) Chapter 3.

31. CEBAF proposal # PR-91-017, D.H. Beck, spokesperson.

32. R. Schiavilla, V. R. Pandharipande, and D. O. Riska, *Phys. Rev.* **C41** (1990)309.

33. D. O. Riska, *Prog. Part. Nucl. Phys.***11** (1984) 199.

34. J. Dubach, J. H. Koch, and T. W. Donnelly, *Nucl. Phys.* **A271** (1976) 279.

35. M. Chemtob and M. Rho, *Nucl. Phys.* **A163** (1971) 1.

36. M. Gari and H. Hyuga, *Nucl. Phys.* **A264** (1976) 409.

37. G. Höhler and E. Pietarinen, *Nucl. Phys.* **B95** (1975) 210.

38. The overal minus sign on the right hand side of Eq. (18) was inadvertantly omitted from Eq. (6) of Ref. [26].

39. D. Berg *et al.*, *Phys. Rev. Lett.* **44** (1980) 706.

40. J. L. Goity and M. J. Musolf, to be published.

41. R. B. Wiringa, R. A. Smith and T. L. Ainsworth, *Phys. Rev.* **C29** (1984) 1207.

42. R. B. Wiringa, *Phys. Rev.* **C43** (1991) 1585.

43. R. B. Wiringa, private communication.

44. R. Schiavilla, V. R. Pandharipande and D. O. Riska, *Phys. Rev.* **C40** (1989) 2294.

45. R. Schiavilla and D. O. Riska, *Phys. Rev.* **C43** (1991) 437.

46. R. Machleidt, Adv. Nucl. Phys. **19** (1989) 1.

47. E. J. Moniz and G. D. Nixon, *Ann. of Phys.* **67** (1971) 58.

Figure Captions

Fig. 1. Two-nucleon (N and N') meson exchange current (MEC) contributions to nuclear matrix elements of the isoscalar EM and strange-quark vector currents. "Pair current" processes, shown in (a,b), arise from the negative energy pole in the intermediate-state, single nucleon propagator. "Transition current" contributions (c) are generated by matrix element of the current operators (indicated by the $\otimes$) between mesonic states (M' and M). As explained in the text, mesonic matrix elements of $J_\mu^{EM}(T=0)$ and $\bar{s}\gamma_\mu s$ vanish when $M' = M$.

Fig. 2. ^{4}He elastic charge form factor, $F_C^{T=0}(q)$. Panel (a) gives the absolute value of the form factor. Circles indicate experimental values. Dashed curve gives theoretical prediction in the impulse approximation (IA) while the solid curve results from the inclusion of two-body currents (IA+MEC). Panel (b) shows individual one- and two-body contributions to $F_C^{T=0}(q)$. One-body contribution is indicatd by solid curve (IA). Dashed curves give contributions from the pionic (circles), ρ-meson (squares), and ω-meson (asterisks) pair currents as well as the ρ-π "transition current (triangles). Short dashed curve indicates the spin-orbit contribution. Only the absolute value of each contribution is plotted, and the signs are indicated in parenthesis. Vector meson pair current contributions are computed including the retardation correction to the charge operator (Eqs. 22c and A.2b).

Fig. 3. Same as Fig. 2, but for the elastic strangeness charge form factor of ^{4}He, $F_C^{(s)}(q)$. In this case, only theoretical predictions are shown, since no measurements have as yet been made. Computations were carried out using $(\rho_s, \mu_s) = (-2.0, -0.2)$, which correspond roughly to the pole model predictions for these parameters [16], and a Galster-like parameterization for the q-dependence of the one-body strangeness form factors. A positive sign for $g_{\rho\pi s}$ was also assumed.

Fig. 4. Elastic strangeness to EM charge form factor ratio, $F_C^{(s)}(q)/F_C^{T=0}(q)$ for different values of nucleon strangeness magnetic moment, μ_s, and fixed strangeness radius, ρ_s.

Fig. 5. Same as Fig. 4, but for fixed μ_s and variable ρ_s. In each case, results using the impulse approximation for $F_C^{(s)}$ are shown along with results including two-body currents for two different choices of sign on $g_{\rho\pi s}$. Panel (a) assumes a large negative value for ρ_s, while panel (b) gives the ratio for vanishing nucleon strangeness radius.

Fig. 6. Prospective constraints on single nucleon strangeness parameters from a 10% measurement of the ^{4}He elastic, PV asymmetry at $Q^2 = -0.6$ $(\mathrm{GeV}/c)^2$. Solid (dashed) lines give the band of allowed values for positive (negative) sign on $g_{\rho\pi s}$. In panel (a), $\lambda_E^{(s)}$ is assumed fixed, while in panel (b), μ_s is held constant. In both panels, central values of $(\rho_s, \mu_s, \lambda_E^{(s)}) = (-2.0, -0.2, 5.6)$ are assumed for purposes of illustration.

Fig. 7. ρ-meson pair current contribution to $F_C^{(s)}(q)$ computed including the retardation correction and omitting it ("#" subscript). Only absolute value is plotted, while sign is indicated in parenthesis.

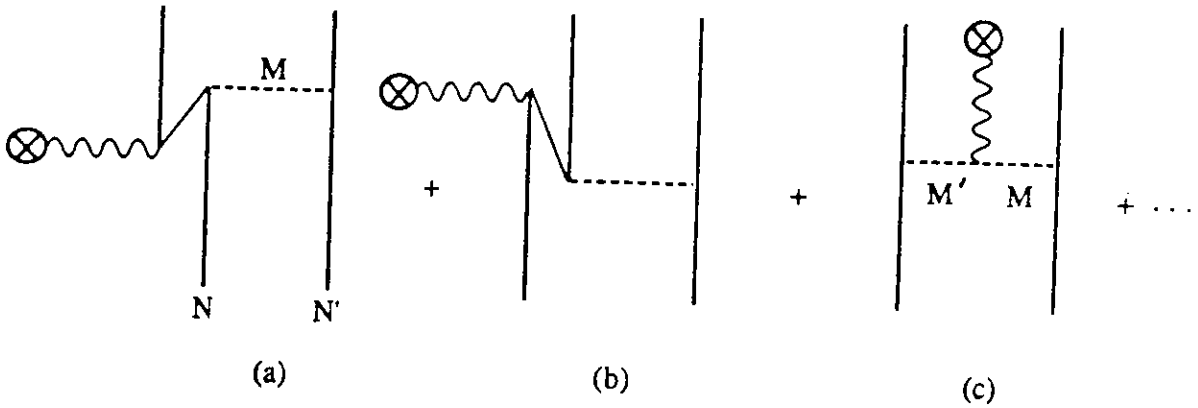

Fig. 1.

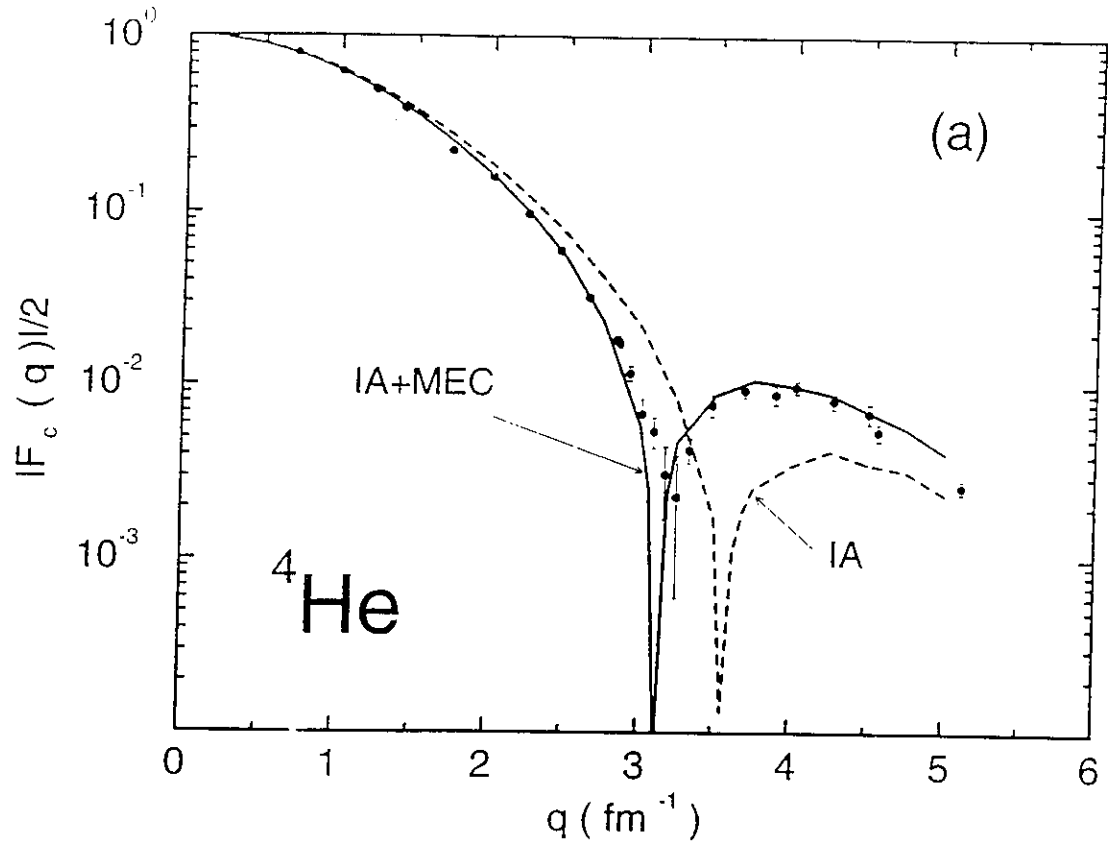
CHARGE FORM FACTOR
(a)
IA+MEC
IA
^{4}He
$|F_c(q)|/2$
q (fm $^{-1}$)

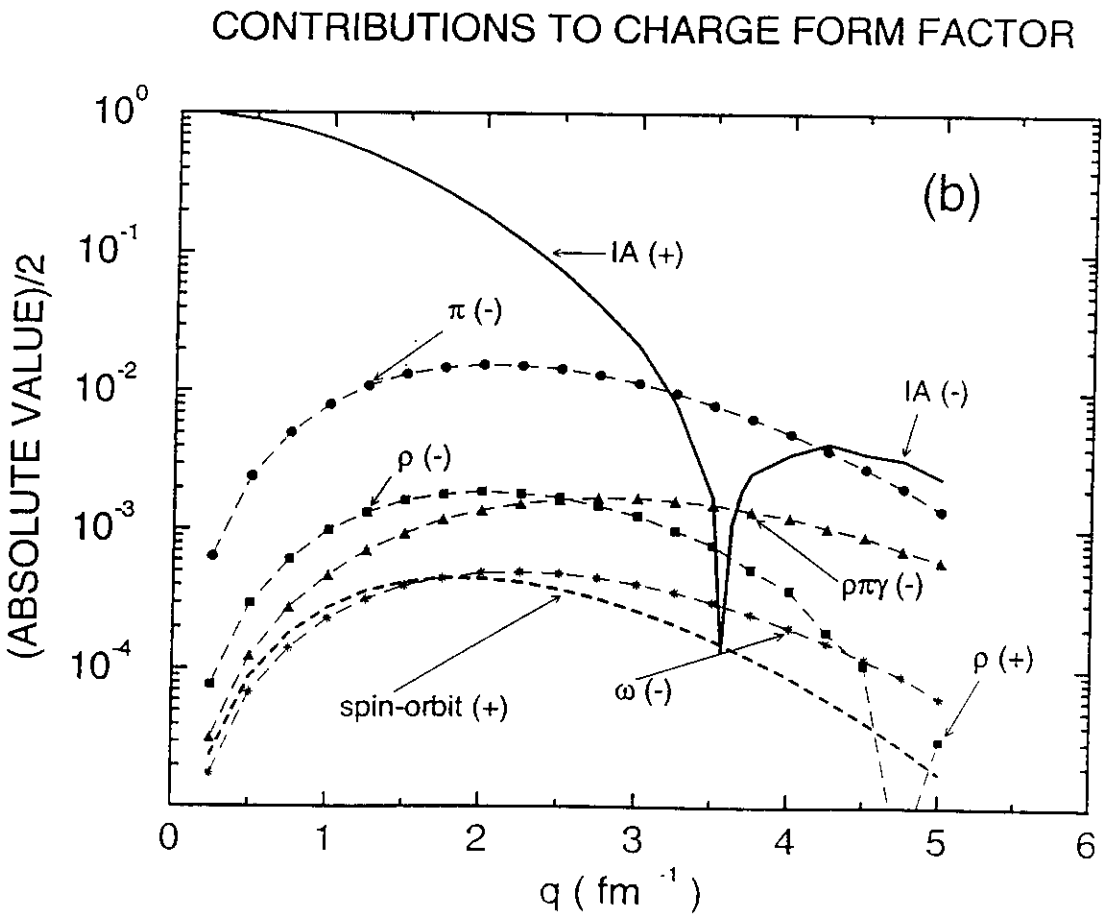
CONTRIBUTIONS TO CHARGE FORM FACTOR
(b)
IA (+)
π (-)
IA (-)
ρ (-)
ρπγ (-)
ρ (+)
ω (-)
spin-orbit (+)
(ABSOLUTE VALUE)/2
q (fm $^{-1}$)

Fig. 2.

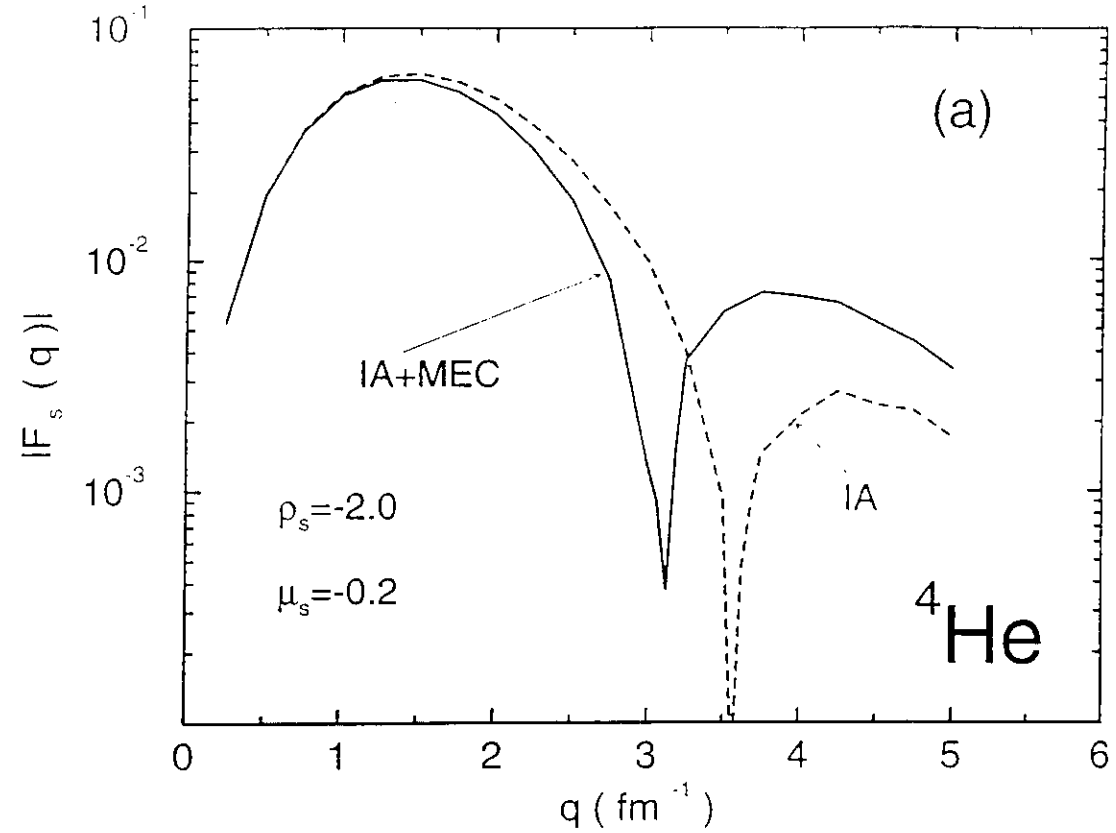
STRANGENESS FORM FACTOR
(a)
IA+MEC
IA
ρ_s=-2.0
μ_s=-0.2
^{4}He
$|F_s(q)|$
q (fm $^{-1}$)

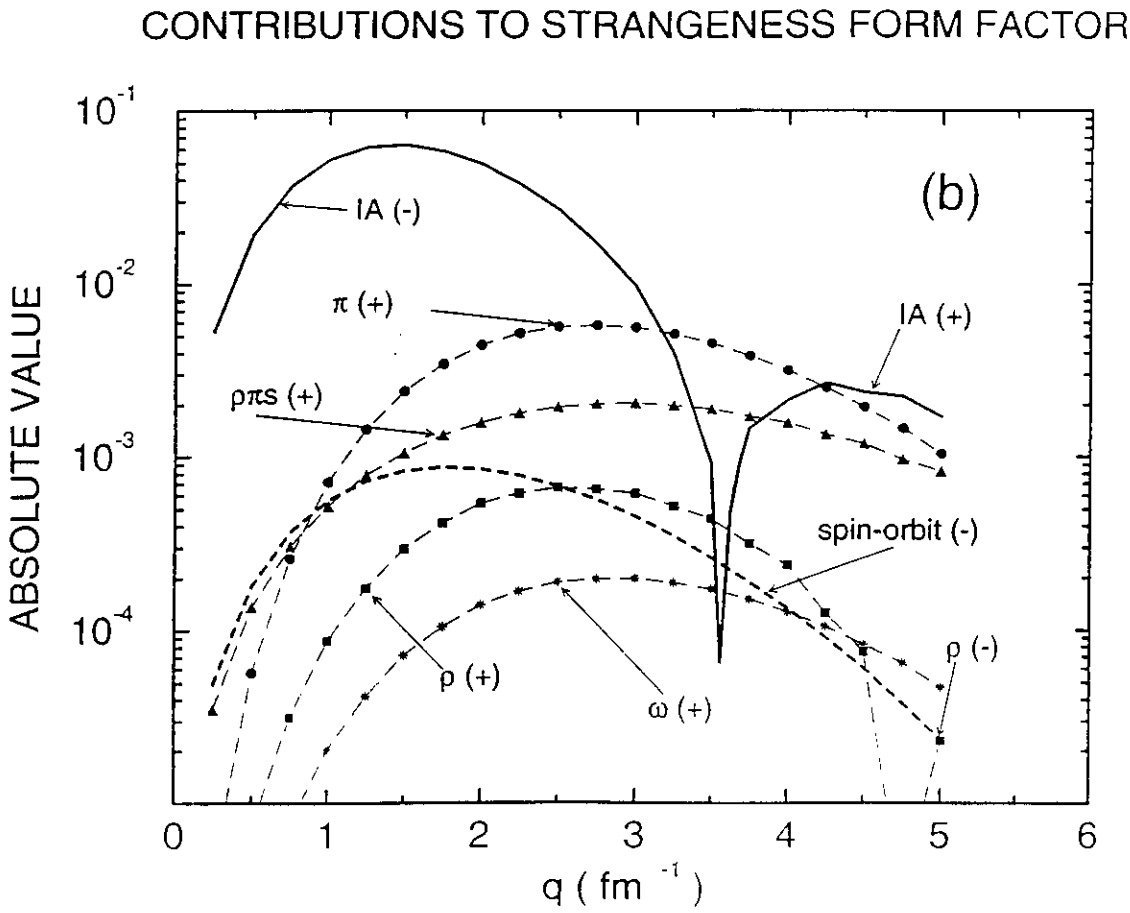
CONTRIBUTIONS TO STRANGENESS FORM FACTOR
(b)
IA (-)
π (+)
IA (+)
ρπs (+)
spin-orbit (-)
ρ (+)
ω (+)
ρ (-)
ABSOLUTE VALUE
q (fm $^{-1}$)

Fig. 3.

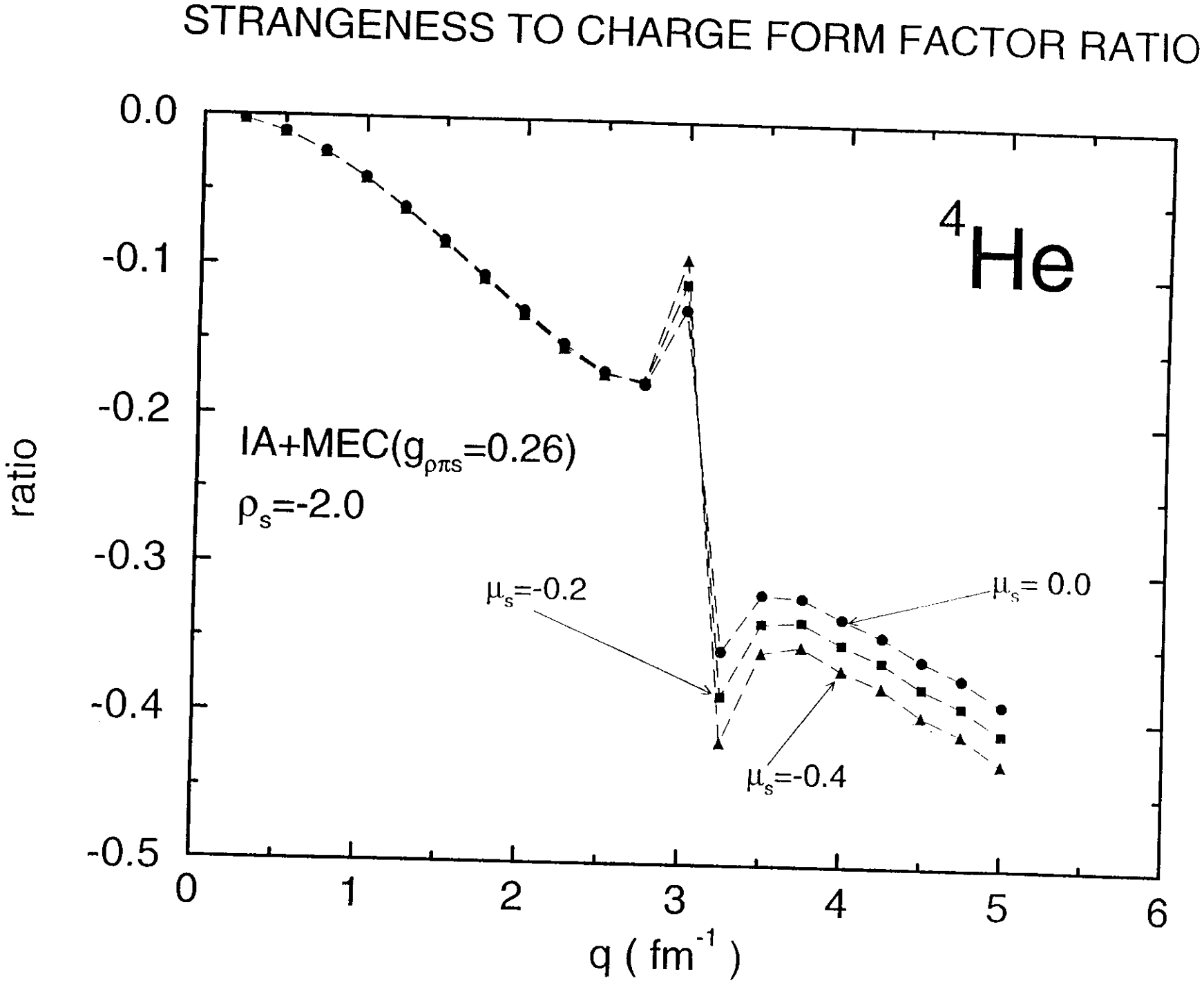
STRANGENESS TO CHARGE FORM FACTOR RATIO
^{4}He
IA+MEC($g_{\rho\pi s}$=0.26)
ρ_s=-2.0
μ_s=-0.2
μ_s= 0.0
μ_s=-0.4
ratio
q (fm^{-1})
0.0
-0.1
-0.2
-0.3
-0.4
-0.5
0
1
2
3
4
5
6

Fig. 4.

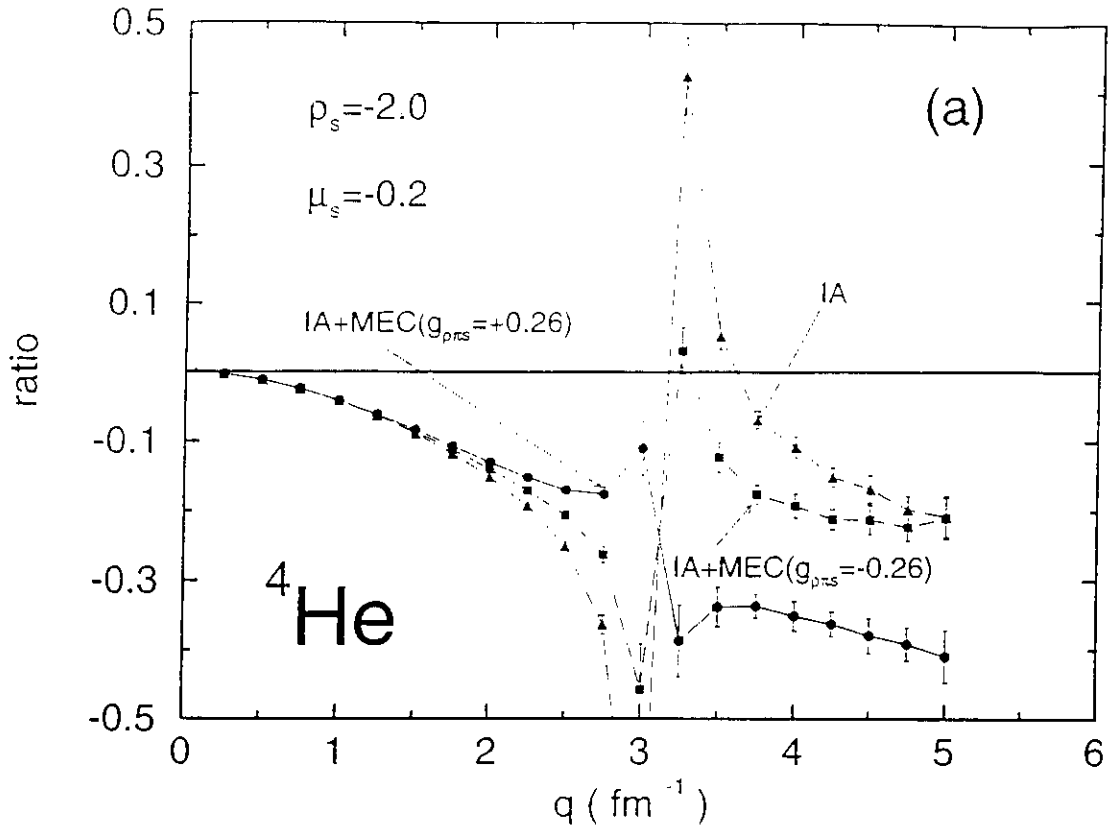
STRANGENESS TO CHARGE FORM FACTOR RATIO
ratio
q (fm $^{-1}$)
ρ_s=-2.0
μ_s=-0.2
(a)
IA
IA+MEC($g_{\rho\pi s}$=+0.26)
IA+MEC($g_{\rho\pi s}$=-0.26)
^{4}He

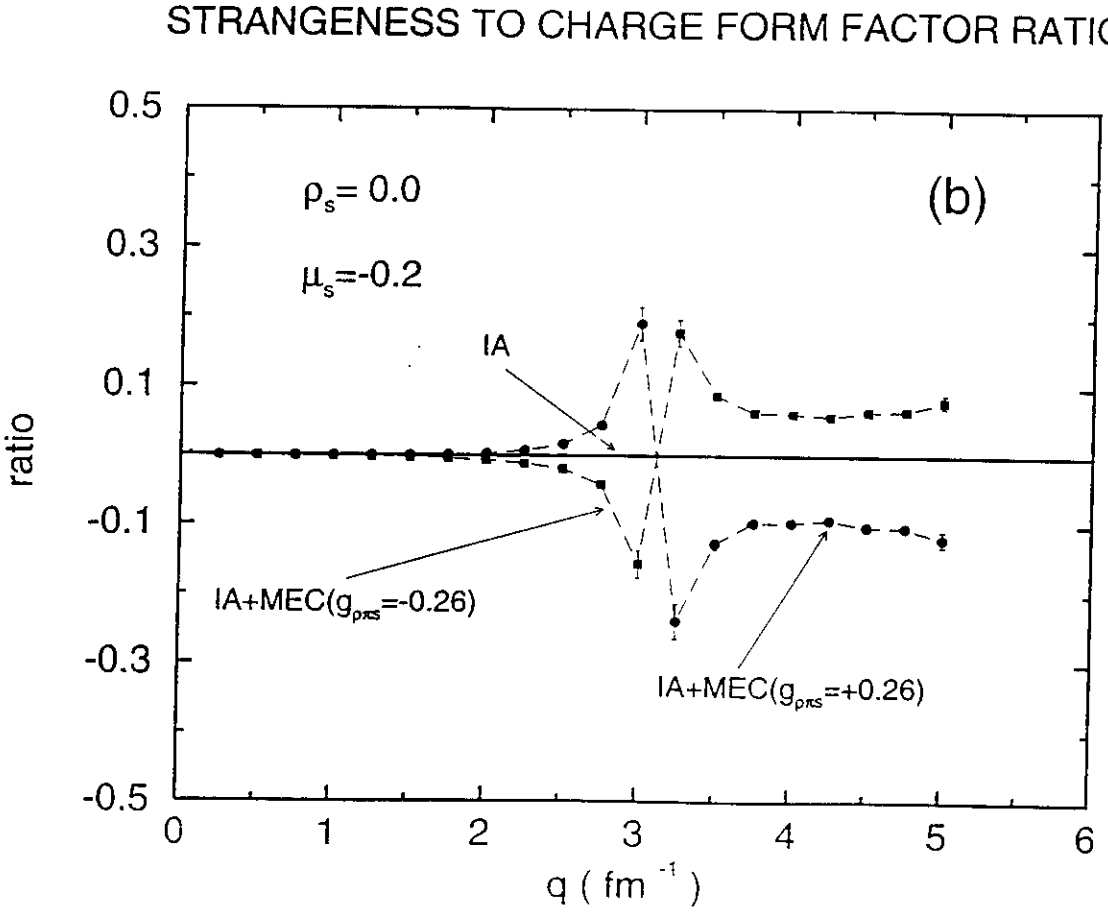
STRANGENESS TO CHARGE FORM FACTOR RATIO
ratio
q (fm $^{-1}$)
ρ_s= 0.0
μ_s=-0.2
(b)
IA
IA+MEC($g_{\rho\pi s}$=-0.26)
IA+MEC($g_{\rho\pi s}$=+0.26)

Fig. 5.

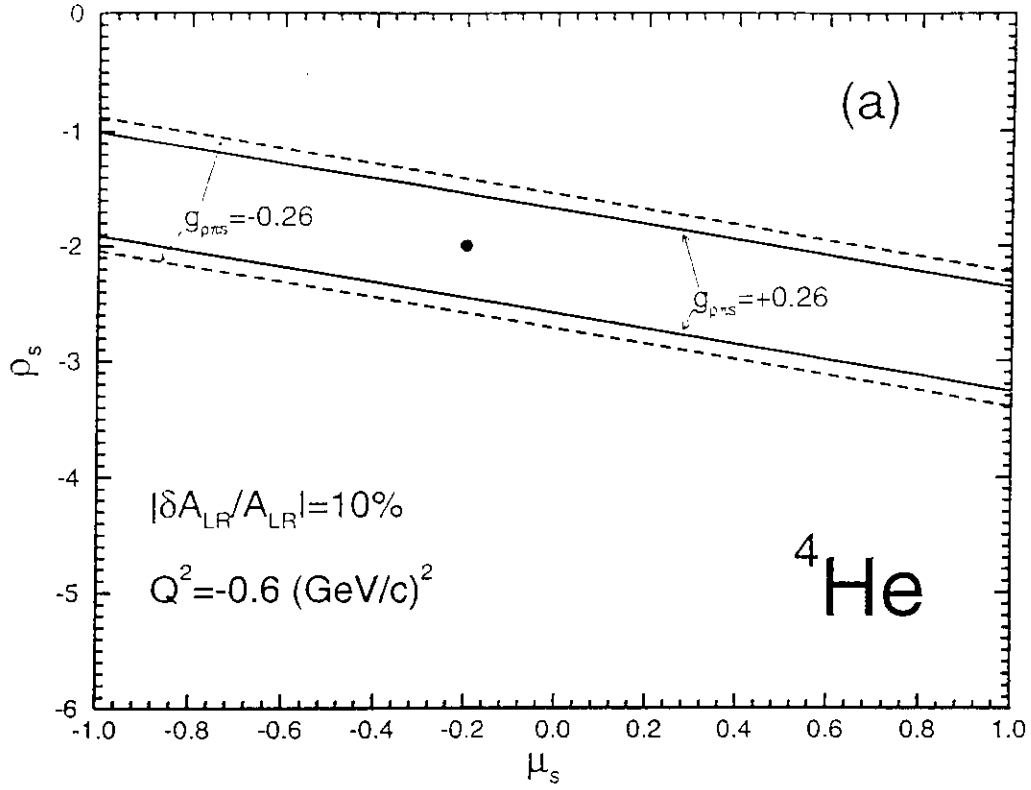
CONSTRAINTS ON $G_E^{(s)}$
(a)
$g_{\rho ns}$=-0.26
$g_{\rho ns}$=+0.26
$|\delta A_{LR}/A_{LR}|$=10%
Q^2=-0.6 (GeV/c)^2
^{4}He
ρ_s
μ_s

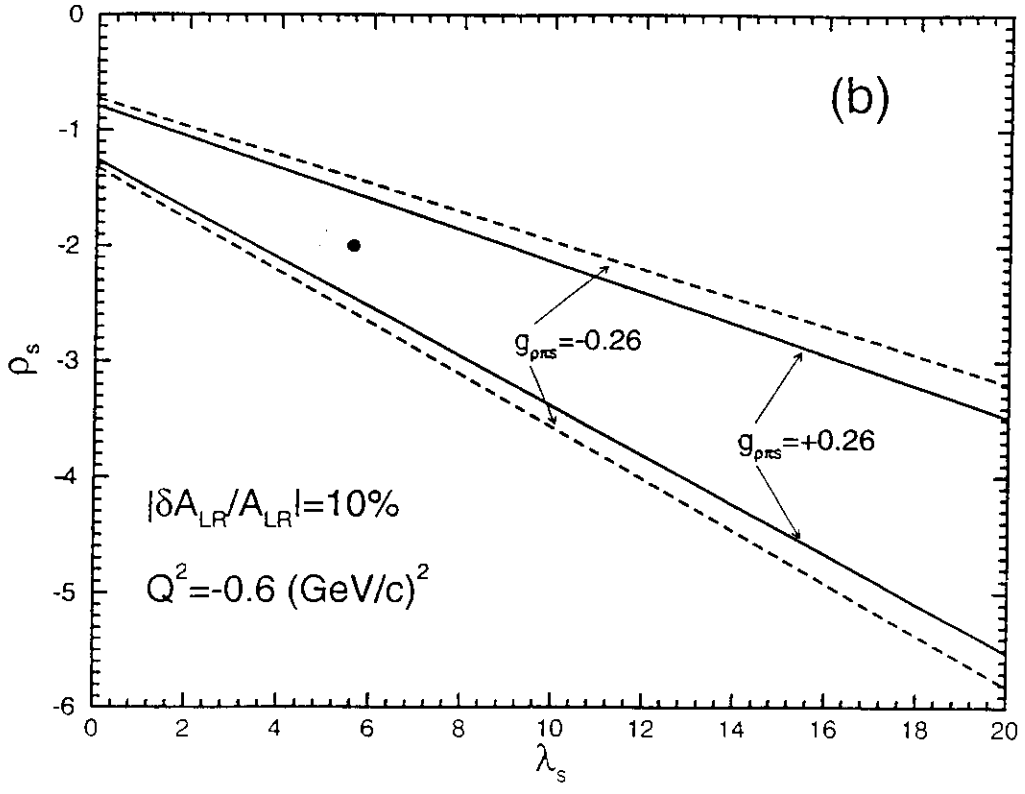
CONSTRAINTS ON $G_E^{(s)}$
(b)
$g_{\rho ns}$=-0.26
$g_{\rho ns}$=+0.26
$|\delta A_{LR}/A_{LR}|$=10%
Q^2=-0.6 (GeV/c)^2
ρ_s
λ_s

Fig. 6.

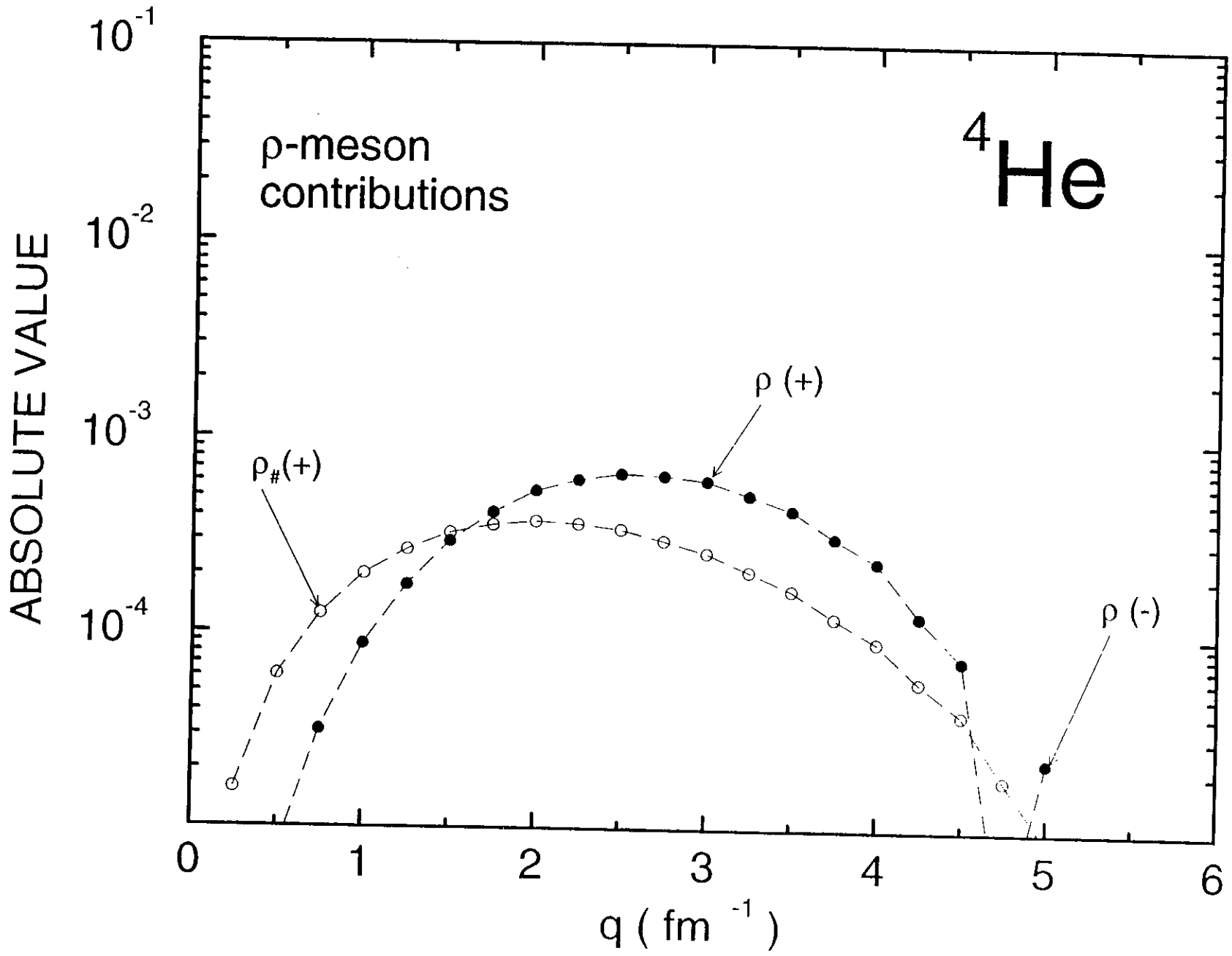
STRANGENESS FORM FACTOR
ρ-meson
contributions
4He
ABSOLUTE VALUE
10-1
10-2
10-3
10-4
ρ#(+)
ρ (+)
ρ (-)
0
1
2
3
4
5
6
q (fm -1)

Fig. 7.